

RESEARCH

Open Access



Comparative enzymatic browning transcriptome analysis of three apple cultivars unravels a conserved regulatory network related to stress responses

F. J. Bielsa^{1,2}, J. Grimplet^{1,2}, P. Irisarri^{1,2}, C. Miranda^{3,4}, P. Errea^{1,2} and A. Pina^{1,2*}

Abstract

Enzymatic browning (EB) endangers the adaptation of apple fruit cultivars to new markets, affecting organoleptic properties and producing economic losses. Polyphenol oxidases and polyphenol compounds play a key role in EB development in apple. However, the regulation of apple response to EB remains to be uncovered. In this study, three apple cultivars with different EB phenotypes ranging from low to high browning in apple pulp were used to study transcriptomic changes over time after fresh cutting (0, 30 and 60 min). This study allowed the identification of 1448 differentially expressed genes (DEGs), revealing both shared and genotype-specific responses, particularly in the affected metabolic pathways associated with EB. At 60 min (T60 vsT0), 77 DEGs were shared by all genotypes, suggesting a conserved regulatory network. This network included genes encoding for protein families such as calcium-binding proteins, heat-shock proteins, redox-responsive transcription factors, WRKY family transcription factors, zinc finger family proteins and disease resistance proteins among others. A co-expressed gene cluster, identified through Weighed Gene Co-Expression Network Analysis (WGCNA), was found to correlate with EB and included 323 genes enriched in several biological terms according to Gene Ontology analysis. Moreover, a more detailed analysis of identified WGCNA gene cluster regulatory sequences allowed the detection of *cis*-regulatory elements belonging to *CAMTA*, *WRKY* and *WUSCHEL* transcription factor families. The identification of these sequences alongside with an abundant and diverse amount of overexpressed transcription factors from various families (*WRKY*, *ERF*, *GRAS*, *GATA*, etc.) point out to a highly regulated stress-response that is strictly connected to innate plant immunity. These findings provide valuable insights into the molecular mechanism involved in apple fresh-cut browning and offer new potential targets for EB regulation.

Keywords RNA-seq, Fresh-cut, WGCNA, *Cis*-regulatory elements, Transcription factor binding sites, Differentially expressed genes, Oxidation, *Malus domestica* × Borkh

*Correspondence:

A. Pina

apina@cita-aragon.es

Full list of author information is available at the end of the article



© The Author(s) 2025. **Open Access** This article is licensed under a Creative Commons Attribution-NonCommercial-NoDerivatives 4.0 International License, which permits any non-commercial use, sharing, distribution and reproduction in any medium or format, as long as you give appropriate credit to the original author(s) and the source, provide a link to the Creative Commons licence, and indicate if you modified the licensed material. You do not have permission under this licence to share adapted material derived from this article or parts of it. The images or other third party material in this article are included in the article's Creative Commons licence, unless indicated otherwise in a credit line to the material. If material is not included in the article's Creative Commons licence and your intended use is not permitted by statutory regulation or exceeds the permitted use, you will need to obtain permission directly from the copyright holder. To view a copy of this licence, visit <http://creativecommons.org/licenses/by-nc-nd/4.0/>.

Background

Malus x domestica Borkh is the second largest fruit product worldwide with an estimated production of 95,83 million tons (MT) in 2022, and the main temperate fruit tree species with an area of 980 kha and production of 18,79 MT at the European level [1]. Besides their great agricultural and economic importance, apples present high nutritional values due to their content of polysaccharides, vitamins, phytosterols and phenolic compounds [2–4] that confer improvements in cardiovascular health, antioxidant activity and even antitumoral activity in humans [2–4]. In recent years, products derived from fresh fruits and vegetables have increased over the past two decades. During this period, ready-to-eat products have emerged as a relevant research field within horticultural science and have opened a new market for apple cultivation [5]. However, apples are prone to browning during fresh-cut, processing, and postharvest storage, which significantly diminishes their appearance, shelf life, taste, flavor, and nutritional value of food products, representing a major economic problem both for the food industry and for consumers [6–9].

Enzymatic browning (EB) of fresh-cut fruit and vegetables is a complex and highly regulated process. During enzymatic browning, polyphenol oxidase (*PPO*) catalyses the oxidation of phenolic compounds in fruits and vegetables, producing quinones. These quinones quickly polymerize, forming dark-coloured pigments [10]. Previous studies have been conducted on enzymatic browning from different species [6, 11, 12] focusing mainly on polyphenol oxidase (*PPO*) acting on phenolic compounds, and antioxidant activity of superoxide dismutases (*SOD*), ascorbate peroxidases (*APX*) and catalases (*CAT*) enzymes [13–15]. However, neither the activity of the browning-related enzymes nor the accumulation of polyphenol substrates is the rate-limiting step in browning development and there is still a lack of consensus on how this process occurs [15]. Zuo et al., [16] has theorized 3 hypotheses that cover previous work on the topic, which explain EB's underlying molecular mechanism based on the regional distribution of phenols and *PPO*, free radical injuries and the protective enzyme system. There, EB can be triggered by many factors and directly compromises cellular integrity. The other metabolic pathways involved include enzymes involved in free radicals scavenging (*SOD*, *CAT*, *APX*), lipid membrane metabolism and phenylpropanoid biosynthesis pathway that has been shown to have an important role during plant response to different stimuli [8, 17].

Enzymatic browning controlling technologies (physical and chemical) have been explored by many research groups [16–18] with different focuses. Physical methods to inhibit *PPO* activity include thermal treatment,

prevention of oxygen exposure, use of low temperature, and irradiation, whereas chemical methods include acidification or reduction using antioxidants chelating agents, or natural extracts [19, 20]. Some of the drawbacks of these anti-browning formulations and processes are that they can only regulate the degree of flesh browning, they are banned from commercialization due to safety concerns, or they increase the production costs of fresh-cut apple slices [10, 19]. The development of non-browning apple cultivar, or the exploitation of traditional varieties can play a great role, through either the direct use of some varieties or by their use in breeding programs.

To date, genetic control of flesh browning has only been partially assessed using the QTL mapping approach, localizing several genomic regions involved in flesh browning. Di Guardo et al. (2013) [14] detected 25 QTLs related to several browning parameters (flesh browning, juice browning, total polyphenols, and polyphenol oxidase activity) in apple, and led to the identification of several genes involved in polyphenol synthesis and cell wall metabolism, showing that *PPO* and *PAL* were most closely related to browning. A QTL for *PPO* activity was detected on chr5, where *PPO* genes are located; and QTLs for total polyphenol content and juice browning were detected on chr16, where leucoanthocyanidin reductase gene is located [21, 22]. Several studies have also described the use of RNA silencing and genome editing to down-regulate *PPO* genes in order to reduce enzymatic browning in potato [23], the browning-resistant Arctic® Apples [24], eggplants [12], and mushrooms [25]. In eggplants, a CRISPR/Cas9-based mutagenesis approach was applied to knock-out three target *PPO* genes in eggplant (*SmelPPO4*, *SmelPPO5*, and *SmelPPO6*), which showed high transcript levels in the fruit after cutting [18].

To advance this knowledge, it is necessary to bring up-to-date molecular biology techniques closer to enzymatic browning research. Among them, transcriptomic and metabolomic analysis are one of such tools that can provide valuable insights into the complex biological networks that underly agronomic traits [26, 27]. Transcriptomics and metabolomic analysis have been successfully applied to elucidate the browning mechanism of fresh-cut potato tubers [28], pear [17, 29], eggplant [12], inhibition by H₂S treatment in fresh-cut apple fruit [30], or to study the internal browning of apples during postharvest storage [6]. However, there are few studies that explore the core regulatory network to comprehensively elucidate the browning mechanism of apple fruit. In this study, we investigated the transcriptomic events involved in enzymatic browning of apple pulp over time (0, 30 and 60 min after flesh cutting) using RNAseq technology. A selection of 3 cultivars with different EB severity was

made from CITA's apple collection and we assessed [1] the transcriptomic profiles during the time course after oxidation, [2] genes differentially expressed among the tested cultivars, [3] the identification of common *cis*-regulatory elements among DEGs, as well as [4] the analysis of a gene clustered associated to EB. Finally, this work provides a comprehensive overview of changes in various metabolic pathways, redox homeostasis genes, stress-related genes and the evaluation of regulatory networks associated with EB. Gaining insights into these mechanisms would provide a great opportunity for developing improved future cultivars and increasing the number of non-browning cultivars would broaden fresh-cut apple availability.

Methods

Plant material and determination of enzymatic browning index of apple cultivars

Representative cultivars were selected to cover the whole range of enzymatic browning severity observed in the apple collection from the Centro de Investigación y Tecnología Agroalimentaria de Aragón (CITA, Zaragoza, Spain) using phenotyping through digital image analysis [31]. Three apple cultivars ranging from low to high enzymatic browning susceptibility were chosen, 'Royal Gala'

represented low-browning cultivars with low phenolic content but commercial interest, whereas 'Borau-01' represented medium-browning cultivars showing moderate phenolic content and are highly overrepresented in our collection. 'Manzana amarilla de octubre' was selected as a high phenolic content cultivar with high associated EB but health related interest and therefore highly valuable for future breeding programs [32] (Fig. 1). Three apple trees were used for collection of 10 fruits per genotype at 5–6 maturity index of Lugol's scale (CTIFL 1–10) and were stored at 2°C for 3–4 weeks until processing to simulate standard postharvest storage practices. These ten fruits were cut into slices of 1 cm thick at room temperature and were used in the oxidation assay. One gram of a pool of apple pieces of all slices was frozen at – 80°C at 3 oxidation times (0 min, 30 min and 60 min) from the outer pulp. Three biological replicates were stored for each time and genotype until use.

Determination of enzymatic browning susceptibility of CITA's apple collection was performed by taking digital images of apple slices at the three oxidation times- These images were evaluated with a homemade-R script to obtain the average colour (in CIELab (1976) L*, a* and b* coordinates) of the entire fruit surface and cluster the studied samples into different groups based on several

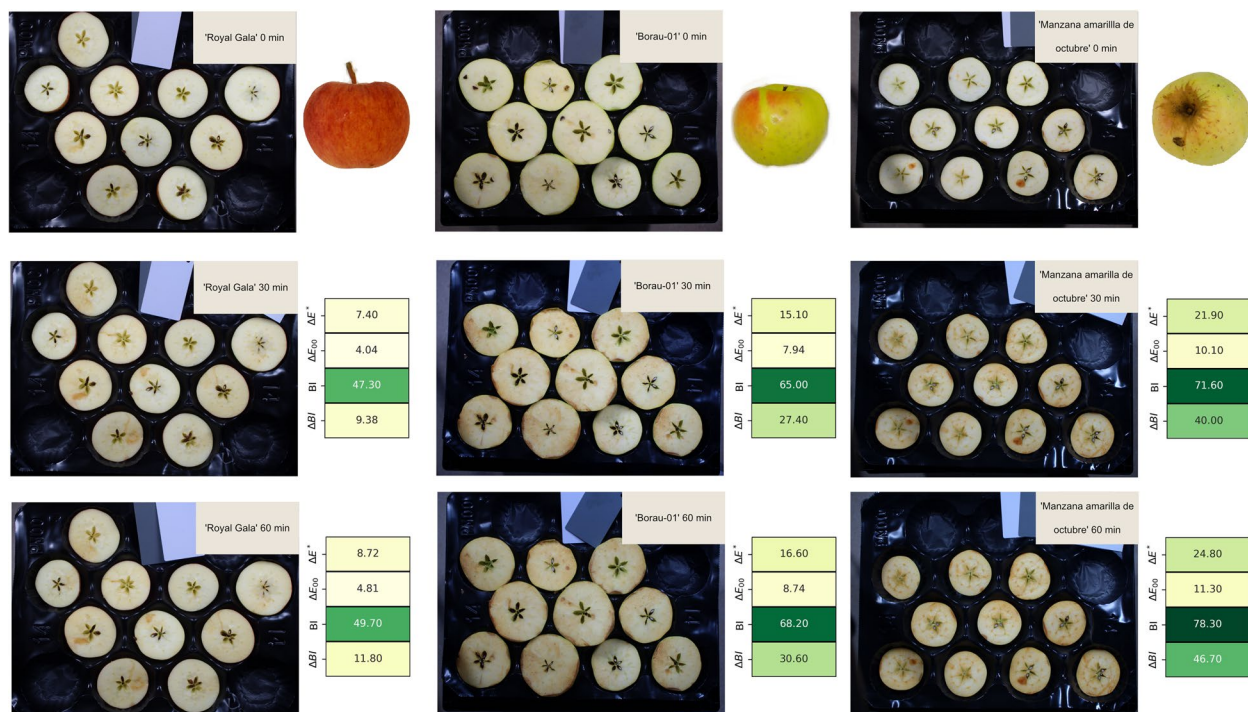


Fig. 1 Apple phenotype from 3 selected cultivars and slices after fresh cutting (top), 30 (middle) and 60 minutes (bottom) after enzymatic browning. Left to right (increasing enzymatic browning susceptibility): 'Royal Gala', 'Borau-01' and 'Manzana amarilla de octubre'. Values are shown for each cultivar and oxidation time for all studied enzymatic browning indexes: BI: Browning Index; ΔBI : Difference in BI from the time of cutting; ΔE^* : Normalized CIE colour difference from the time of cutting; ΔE_{00} : CIEDE2000 colour difference from the time of cutting

enzymatic browning indexes [31]. The suitability of four enzymatic browning indexes (BI, ΔBI , ΔE_{00} , ΔE^*) previously calculated for each genotype was evaluated based on correlation to transcriptome analysis results.

Browning Index (BI), according to the method of Palou et al. [33]:

$$BI = [100(x - 0.310)]/0.172 \quad (1)$$

where

$$x = (a^* + 1.75L^*) / (5.645L^* + a^* - 3.012b^*) \quad (2)$$

Difference in BI (ΔBI) from the time of cutting as

$$\Delta BI = BI_0 - BI_t \quad (3)$$

Normalized CIE colour difference (ΔE^*) from the time of cutting as

$$\Delta E^* = \sqrt{(L_t^* - L_0^*)^2 + (a_t^* - a_0^*)^2 + (b_t^* - b_0^*)^2} \quad (4)$$

CIEDE2000 [34] colour difference (ΔE_{00}) from the time of cutting defined as

$$\Delta E_{00} = \sqrt{\left(\frac{\Delta L'}{k_L S_L}\right)^2 + \left(\frac{\Delta C'}{k_C S_C}\right)^2 + \left(\frac{\Delta H'}{k_H S_H}\right)^2 + R_T \left(\frac{\Delta C'}{k_C S_C}\right) \left(\frac{\Delta H'}{k_H S_H}\right)} \quad (5)$$

and calculated according to expressions described in Sharma et al. [35], by means of the package *ColorNameR* [36].

RNA extraction and sequencing

RNA extraction was performed using 1 g of ground apple pulp in a mortar in liquid Nitrogen followed by CTAB-SEVAG protocol adapted by Meisel [37] with some modifications to optimize RNA concentration and quality. RNA integrity was checked with a 1% agarose gel electrophoresis and genomic DNA was removed following TURBO DNA-free kit protocol (Invitrogen, Thermo Fisher scientific). Samples' RNA concentration was determined using Qubit BR (Thermo Fisher) and quality control was performed with a Bioanalyzer 6000 nano (Agilent Technologies) at Centro Nacional de Análisis Genómico (CNAG, Barcelona, Spain). All samples used in the experiment had a RIN quality control value >7.1 (Table S1) and the transcriptomic experiment was performed in triplicate. Following library preparation, sequencing was performed with an Illumina Novaseq 6000 S1 system (Illumina, USA) with >50 M of reads per sample and a read length of 2×100 bp stranded mRNA.

Raw data FastQ files were processed using Galaxy platform (Galaxy version 1.0.0), each sample's files were converted to fastqsanger format and files from each biological

sample were concatenated using Concatenate Datasets (Galaxy version 1.0.0). Forward and reverse files of each sample were coupled, and dataset were processed as a list of paired-end reads using Galaxy tool 'build list of pairs' (Galaxy version 1.0.0). Quality control of paired-end pairs was performed using FastQC (Galaxy version 0.73 + galaxy0). After confirming that quality standards were met (no 3' and 5' degradation, normal GC%, no excessive duplicated reads), adapter sequences and low-quality (Q20) base pair were removed using Trimmomatic (Galaxy version 0.38.1) [38]. A total of twenty-seven samples were then aligned using HISAT 2 (Galaxy version 2.2.1 + galaxy0) [39] to GDDH13 Golden Delicious reference genome v1.1 [40] with a minimum intron length of 20 bp and a maximum intron length of 20,000 bp, and selecting stranded mRNA data. Samples were then checked for duplicates using 'Mark duplicates' (Galaxy version 2.18.2.4), sample 's pairs were synced using 'Fixmate Information' (Galaxy Version 2.18.2.2) and arranged into groups of replicates with 'add or replace read groups' from Picard Tools (Galaxy version 2.18.2) (<http://broadinstitute.github.io/picard/>). Additionally, sample reads were

sorted by their corresponding annotated gene name using Samtools sort (Galaxy version 2.0.4) [41]. Gene annotation file from 'GDDH13 Golden Delicious reference genome v1.1' was chosen to estimate read counts using featureCounts (Galaxy version 2.0.1 + galaxy2) on twenty-seven samples. Finally, ColumnJoin (Galaxy version 0.0.3) was used to merge the output files, and edgeR (Galaxy version 3.36.0 + galaxy0) [42] was used to calculate gene expression changes between times among samples.

Data was further processed using Python scripts in Spyder IDE (Version 5) to select DEGs, GO term annotation and other data treatment-related processes. DEGs were defined as genes with a $|\log_2 FC|$ greater than 1 and a false discovery rate (FDR) less than 0.05. A gene ontology analysis was performed using GoEnrichment (Galaxy Version 2.0.1).

Weighed gene co-expression network analysis

To perform analysis of relationships between genes and their correlation to enzymatic browning, raw reads were filtered removing genes with no expression. CountsPerMillion were calculated and transformed into logCPM values and a filter was applied selecting genes with a logCPM value greater than 0.05 for at least 3 of the biological replicates of an individual and oxidation time. WGCNA was performed using

WGCNA R package [43] following software authors' guidelines. To ensure identification of co-expressed modules without directionality constraints in gene–gene correlations, we selected an 'unsigned' TOM matrix. Free-scale topology of the matrix was achieved when selecting power = 24. Moreover, minModuleSize parameter was set at 30, as the minimal number of genes to constitute a module, and an additional parameter maxBlockSize was set at 45,000 to avoid segmentation of data for further algorithm calculations. Correlation with phenotypic traits was done using Pearson's correlation test with p-value < 0.05. Gene Modules correlated with EB were used to find top hubs among our genes using 'intramodularConnectivity' (WGCNA R package), which showed the highest interconnectivity values.

Characterization of promoter sequences of enzymatic browning correlated genes

The detection and the analysis of *cis*-regulatory elements in upstream genomic sequences of a gene module associated with enzymatic browning were evaluated using RSAT (Regulatory Sequence Analysis Tools) [44] following the methodology of Contreras-Moreira [45], to identify common Transcription Factor Binding Sites (TFBSs). Briefly, upstream sequences were retrieved and analysed using peak motif detection to look for common motifs in WGCNA gene cluster. Found motifs were further tested for significance using a pool of random sequences of similar length and results were analysed as previously described [46].

Quantitative Real-Time PCR (qRT-PCR) analysis

Gene expression analysis of 8 DEGs was performed in a StepOnePlus™ Real-Time PCR System (Applied Biosystems™). A final volumen of 10 μ L (10 ng cDNA, 0.3 μ M Forward Primer, 0.3 μ M Reverse Primer, 5 μ L iTaq™ Universal SYBR® GREEN Supermix (Biorad) 2 \times and RT-PCR grade water) was used for the reaction with the following steps for all primers set (Table S2): A first denaturation step at 95°C for 4 min; 40 cycles of: denaturation at 95°C for 30 s, an hybridization step at 62°C for 1 min and an elongation step at 72°C 1 min; a final elongation step at 72°C for 10 min. Melting curve was performed with a first step of hybridization at 62 °C followed by a gradual temperature increment of +0.5 °C/s until reaching 95°C to check dimer formation of primers. ΔR_n values were obtained from StepOne Plus results and analysed using LinRegPCR to determine PCR efficiency [47]. The relative expression level was calculated using the comparative $2^{-\Delta\Delta C_t}$ method [48]. Four technical replications for each of the 3 biological replicates were performed.

Statistical analyses

To identify statistically significant differences in the expression of EB-related genes (e.g., *SOD*, *CAT*, *APX*, *PPO*, *PAL*), logCPM data for these genes were analysed using a one-way Analysis of Variance (ANOVA). This approach was employed to evaluate whether gene expression levels varied significantly across the studied cultivars. The effect of cultivar on each gene's expression was assessed using an ordinary least squares (OLS) model. When ANOVA results indicated a significant effect (p < 0.05), a post-hoc Tukey's Honestly Significant Difference (HSD) test was conducted to determine which pairs of cultivars exhibited significant differences in their mean constitutive expression levels.

Results

Phenotypic characteristics and high throughput sequencing and assembly

The high ('Manzana amarilla de octubre'), the medium 'Borau- 01' and the low ('Royal Gala') browning phenotypes showed different degrees of browning within the treatment times (30, 60 min after fresh cutting) (Fig. 1). To compare the flesh browning variation among the three cultivars over time, four enzymatic browning indexes were determined (BI, Δ BI, Δ E00, Δ E*). The high browning cultivar 'Manzana amarilla de Octubre' had a more pronounced browning index (BI₆₀ = 78.30) compared with the intermediate (BI₆₀ = 68.20) and low browning cultivars slices (BI₆₀ = 49.70). RNA libraries were generated with these 3 cultivars with different EB severity.

A total of 2.064 million raw sequence reads were generated using the Illumina Novaseq 6000 S1 sequencing platform. After adapter removal and alignment to the apple reference genome [40] using HISAT2 (Galaxy version 2.2.1 + galaxy0) an overall alignment rate of 95.45% was obtained among our samples (Table S1).

From the 52,741 annotated genes in reference genome 'GDDH13 Golden Delicious reference genome v1.1', 33,661 were expressed in the RNAseq data after filtration of logCPM data analysis. Analysis of expression levels between transcripts expressed at T60 vsT0 and T30 vsT0 oxidation times allowed the identification of a total of 1448 genes differentially expressed in our samples among which 799 were unique (Table S3).

DEGs during enzymatic browning

Transcriptomic analysis of gene expression of apple pulp during enzymatic browning revealed differences between the three genotypes with different degrees of enzymatic browning severity, pointing out a genotype-dependent response to oxidation. Identification of DEGs at different oxidation times showed significant differences between cultivars and at two time points within cultivars (Table 1).

Table 1 DEGs per time comparison and cultivar

Cultivar	Time comparison	Up-Regulated DEGS (FDR < 0.05)	Down-regulated DEGS (FDR < 0.05)
'Royal Gala'	30 min vs 0 min	198	15
	60 min vs 0 min	526	74
'Borau- 01'	30 min vs 0 min	1	1
	60 min vs 0 min	101	6
'Manzana amarilla de octubre'	30 min vs 0 min	60	0
	60 min vs 0 min	445	21
TOTAL		1331	117

Number of up and down regulated DEGs found in 'Royal Gala' (low browning susceptibility), 'Borau- 01' (medium browning susceptibility), 'Manzana amarilla de octubre' (high browning susceptibility), with different enzymatic browning severity at 30 and 60 min of oxidation

'Royal Gala' showed a higher number of DEGs to enzymatic browning with 526 up-regulated genes and 74 down-regulated genes at 60 min of oxidation compared to T0 (T60 vsT0). In contrast, 'Borau- 01' showed no response at 30 min of oxidation (T30 vsT0) and showed a lower number of DEGs at 60 min in comparison to 'Manzana amarilla de octubre' and 'Royal Gala' (Table 1). Our results showed a general increase in the number of genes affected by a change of expression until 60 min for all cultivars in which up-regulated genes are more abundant than down-regulated genes (Table 1).

DEGs showed a great heterogeneity of $|\log_2FC|$ values (Table S3). Several genes showed changes in expression greater than $|\log_2FC| > 5$ especially in 'Royal Gala' (T60 vsT0: 57, T30 vsT0: 10) and 'Manzana amarilla de octubre' (T60 vsT0: 72, T30-T0:11) (Table S3).

Most up-regulated genes with higher $|\log_2FC|$ values belong to families involved in signal transduction, protein ubiquitination, degradation and transcription regulation (Table S3). Some of these top genes are shared by 'Royal Gala' and 'Manzana amarilla de octubre', such as genes belonging to ERF family (MD10G1094700 and MD05G1080900), two redox-responsive transcription factors), protein ubiquitination proteins (MD12G1040900, a plant-U-box) or other transcription factor protein families (MD02G1096500, an integrase-type DNA-binding superfamily protein) (Table 2, Table S3). The downregulated genes observed in 'Borau- 01' encoded a 'Rhamnogalacturonate lyase family protein' (MD01G1043300) and a 'DNAJ heat shock N-terminal domain-containing protein' (MD14G1156300).

Although differences in the number of genes are evident among all cultivars at both oxidation times, especially at 30 min, a conserved response to enzymatic browning has been found in the three apple cultivars (Fig. 2A). At 30 min (T30 vsT0), only one gene was

shared by all genotypes (MD09G1262900, a calcium-binding EF-hand family protein) which was up-regulated. However, 'Borau- 01' showed a weaker response due to an unknown factor, whereas 'Royal Gala' and 'Manzana amarilla de octubre', low and high browning phenotypes, shared 51 DEGs at 30 min (Fig. 2A). Furthermore, 77 DEGs were shared by all genotypes (Fig. 2B) at 60 min (T60 vsT0), whereas low and high browning phenotypes shared 211 DEGs. The gene pool associated with the 'conserved' response of apple pulp to enzymatic browning at 60 min comprises a heterogeneous group of DEGs coding for protein families such as calcium-binding proteins, heat-shock proteins, redox-responsive transcription factors, WRKY family transcription factors, zinc finger family proteins and disease resistance proteins among others (Fig. 3). The calcium-binding EF-hand family protein gene (MD09G1262900) shared at 30 min (T30 vsT0) was also found in this pool at 60 min (T60 vsT0), along with the previously mentioned MD10G1094700 and MD05G1080900, two redox-responsive transcription factors also known as ethylene responsive factors (*AP2/ERF*), which showed some of the highest changes in expression among all genes (Table S3). To validate the RNA-seq results, we performed qRT-PCR expression analysis on 8 apple genes. There was no significant difference between qRT-PCR analysis results and RNA-seq data and similar trends were observed in up-regulated genes selected. As shown in Figure S1, correlation analysis of the gene expression ratios showed a good correlation ($R^2 = 0.846$) between qRT-PCR and RNASeq, indicating the high reliability of the RNA-Seq data obtained in our study.

Functional categories of differentially expressed genes

To understand what biological processes are implicated in response to enzymatic browning, we assigned the DEGs to known Gene Ontology (GO) categories. Among 799 unique genes differentially expressed in the samples studied, 412 unique (51.56%) DEGs were assigned to three ontology classes, Molecular Function, Biological Process and Cellular Component categories for all cultivars (Table S4, Fig. 4). Molecular Function enriched terms contained genes involved in 'DNA binding' (GO:0003677), 'protein phosphorylation' (GO:0004672, GO:0004713), 'DNA-binding transcription factor activity' (GO:0003700), another post-transcriptional regulation processes such as 'ubiquitination' (GO:0004842) and 'cleavage' (GO:0140096) (Fig. 4A, Table S4). These enriched terms were more abundant in 'Royal Gala' and 'Manzana amarilla de octubre' than 'Borau- 01' at both times, although medium browning phenotype also showed some enriched terms at 60 min (Fig. 4A).

Table 2 Top 5 DEGs with the highest $|\log_2FC|$ value in each sample. Annotation was obtained from GDDH13 GFF Golden Delicious v1 ([40])

Cultivar	Oxidation time (min)	GeneID	$ \log_2FC $	FDR	Annotation
'Royal Gala'	30 vs 0 Minutes	MD02G1096500	9,9	5,93E- 05	Integrase-type DNA-binding superfamily protein
		MD05G1080900	7,77	2,89E- 10	redox responsive transcription factor 1
		MD10G1094700	6,92	1,52E- 04	redox responsive transcription factor 1
		MD14G1123000	6,47	6,68E- 05	WRKY family transcription factor
		MD10G1150400	6,06	3,32E- 03	ARF-GAP domain 11
	60 vs 0 Minutes	MD02G1096500	10,94	4,57E- 06	Integrase-type DNA-binding superfamily protein
		MD10G1094700	9,35	1,97E- 07	redox responsive transcription factor 1
		MD05G1080900	9,12	8,25E- 12	redox responsive transcription factor 1
		MD10G1150400	8,25	2,99E- 06	ARF-GAP domain 11
		MD12G1040900	7,94	3,48E- 03	plant U-box 23
'Borau- 01'	30 vs 0 Minutes	MD09G1262900	1,48	3,14E- 02	Calcium-binding EF-hand family protein
		MD14G1156300	- 1,16	3,14E- 02	DNAJ heat shock N-terminal domain-containing protein
	60 vs 0 Minutes	MD01G1043300	- 7,22	3,67E- 02	Rhamnogalacturonate lyase family protein
		MD05G1080900	7,1	3,90E- 09	redox responsive transcription factor 1
		MD10G1094700	6,54	3,47E- 03	redox responsive transcription factor 1
		MD09G1039300	4,59	5,20E- 07	zinc finger (AN1-like) family protein
		MD13G1251000	4,44	5,11E- 03	lectin protein kinase family protein
'Manzana amarilla de octubre'	30 vs 0 Minutes	MD15G1221100	8,55	2,18E- 05	Integrase-type DNA-binding superfamily protein
		MD05G1080900	8,32	4,22E- 09	redox responsive transcription factor 1
		MD02G1096500	8	3,27E- 02	Integrase-type DNA-binding superfamily protein
		MD01G1196100	7,88	2,44E- 02	C-repeat/DRE binding factor 2
	60 vs 0 Minutes	MD14G1123000	6,96	1,29E- 03	WRKY family transcription factor
		MD02G1096500	11,47	4,87E- 06	Integrase-type DNA-binding superfamily protein
		MD05G1080900	11,04	2,53E- 12	redox responsive transcription factor 1
		MD12G1040900	11,01	9,73E- 04	plant U-box 23
		MD01G1196100	10,91	4,87E- 06	C-repeat/DRE binding factor 2
		MD12G1133300	10,6	2,67E- 06	exocyst subunit exo70 family protein H4

'Royal Gala' and 'Manzana amarilla de octubre' also showed shared enriched terms in the Biological Process category at 60 min (Fig. 4B). However, all 3 cultivars showed different enriched terms highlighting the various gene pools involved in each response. Some of these terms related to stress (GO:0006950) and heat response (GO:0009408) displayed a group of genes that were only present in 'Manzana amarilla de octubre' at 60 min including different proteins such as heat shock transcription factor A2 (MD15G1057700), heat shock transcription factor A3 (MD14G1015900), heat shock transcription factor A6B (MD03G1258300) or winged-helix DNA-binding transcription factor family proteins (MD09G1233700, MD04G1017400, MD04G1064700). Furthermore, 'Borau- 01' showed a 'chorismite metabolic process' (GO:0046417) term enriched which is crucial for secondary metabolism and one corresponding gene was also differentially expressed in 'Royal Gala' and 'Manzana amarilla de octubre' (Chorismate mutase 2, MD15G1040000) (Fig. 4B). At 60 min, 'Royal Gala'

also showed a significantly enriched term related to 'nitrate assimilation' (GO:0042128), which could be crucial for glutathione regeneration through cell nitrogen uptake and glutamine synthesis (MD15G1357900 and MD08G1172400).

The Cellular Component category also revealed enriched terms for 'Manzana amarilla de octubre' at 30 and 60 min, and 'Royal Gala' at 60 min. Both cultivars shared a term related to ubiquitin ligase complex (GO:0000151), which plays a fundamental role in protein cleavage through proteasome degradation. Additionally, 'Manzana amarilla de octubre' exhibited two specific terms related to cell wall (GO:0005618) and apoplast (GO:0048046), which could highlight a stronger wounding-healing response (Fig. 4C). Overall, differences in Gene ontology enriched terms have provided some novel insights regarding the molecular mechanisms associated with enzymatic browning, useful for a better understanding of the temporal expression of genes in response to oxidation.

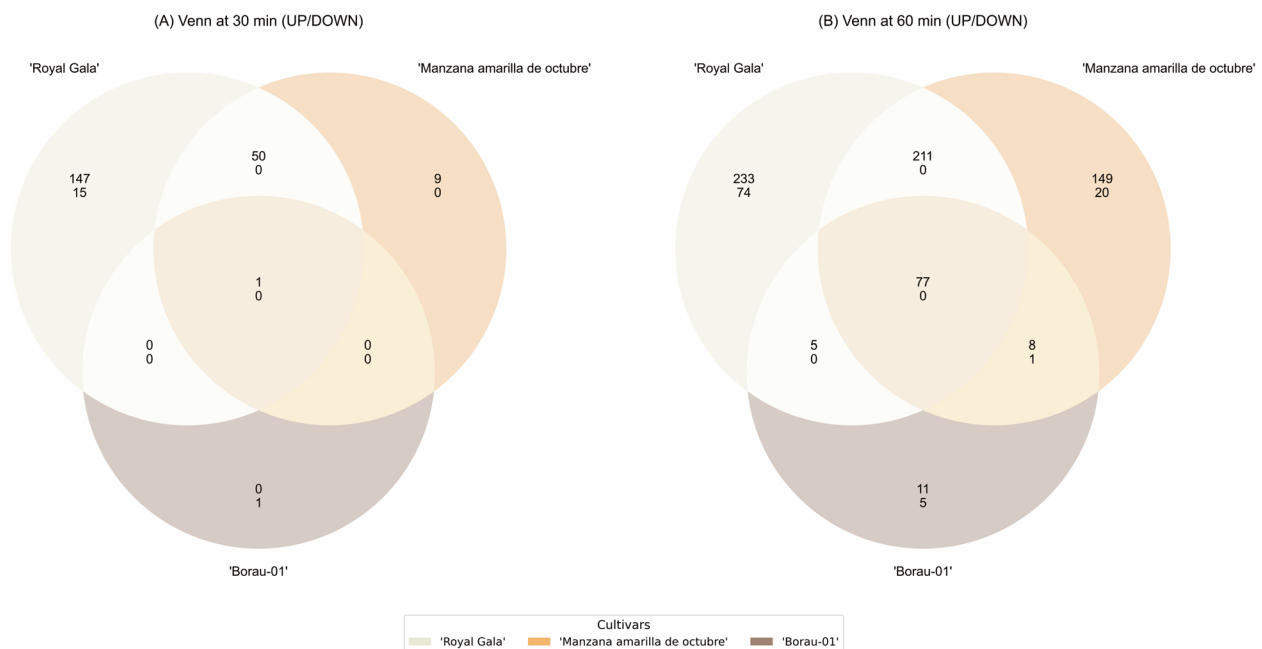


Fig. 2 Venn diagram of DEGs at 30 (A) and 60 min (B) of oxidation of 'Royal Gala', 'Borau-01' and 'Manzana amarilla de octubre'. Up and down-regulated shared number of genes are represented vertically in each intersection

Enzymatic browning-related genes

Phenylpropanoid biosynthesis pathway enzymes related genes *PPO* and *PAL* and antioxidant enzymes such as *SOD*, *CAT* or *APX* have been related to phenotype susceptibility during enzymatic browning. In this study, we have found several differences in the constitutive expression of these genes among cultivars and changes in gene expression through time. Six *PAL*-annotated genes in GDDH13 reference genome were expressed in the studied samples and constitutive expression of these genes was significantly higher in 'Manzana amarilla de octubre' and 'Borau-01' compared to 'Royal Gala' (Fig. 5A). Therefore, the enzymatic browning severity in these three cultivars appears to be influenced by the phenylpropanoid pathway key enzyme *PAL*, which determines phenolic concentration. Likewise, differential expression analysis of 18 *PPO* annotated genes revealed that none of the cultivars showed expression changes of *PPO* during apple pulp enzymatic browning in our samples. However, among 9 expressed *PPO*s, a significant difference ($p < 0.05$) between cultivar *PPO* constitutive expression was found for 5 of these genes (MD05G1318900, MD10G1298200, MD10G1298700, MD10G1299100, MD10G1299300) among the cultivars. Notably, the medium-browning phenotype 'Borau-01' displayed higher constitutive expression of these genes (Fig. 5B).

Regarding the expression of the antioxidant enzymes, among 3 annotated catalases under the name

'catalase-2', two appear to have a significant constitutive difference between cultivars, whose higher value corresponds to 'Manzana amarilla de octubre' (Figure S2). Likewise, several metal ion binding *SOD* have been found to differ in constitutive levels of expression of these cultivars. 'Manzana amarilla de octubre' had lower expression of one 'Fe superoxide dismutase gene' (MD13G1005800) compared to 'Royal Gala' and 'Borau-01', whereas 'Royal Gala' mostly showed a higher constitutive expression of 'copper/zinc superoxide dismutases', whose expression is quite heterogeneous among 'Manzana amarilla de octubre' and 'Borau-01' (Figure S2). Finally, ascorbic acid cycle is a fundamental key in ROS scavenging in stress response processes and involves several enzymes such as ascorbate peroxidase (*APX*), monodehydroascorbate reductase (*MDHAR*) or dehydroascorbate reductase (*DHAR*). Analysis of expression levels of these enzyme-encoding genes revealed an irregular expression pattern in constitutive levels among the cultivars (Figure S2). Therefore, it cannot be said that any of these varieties has a higher level of expression of these genes. Moreover, none of the *APX* encoding genes showed changes through time, although a nucleobase-ascorbate transporter (MD03G1135100, nucleobase-ascorbate transporter 12) with a $|\log_2FC| = 1.02$ was found at 60 min in 'Royal Gala' (Table S3).

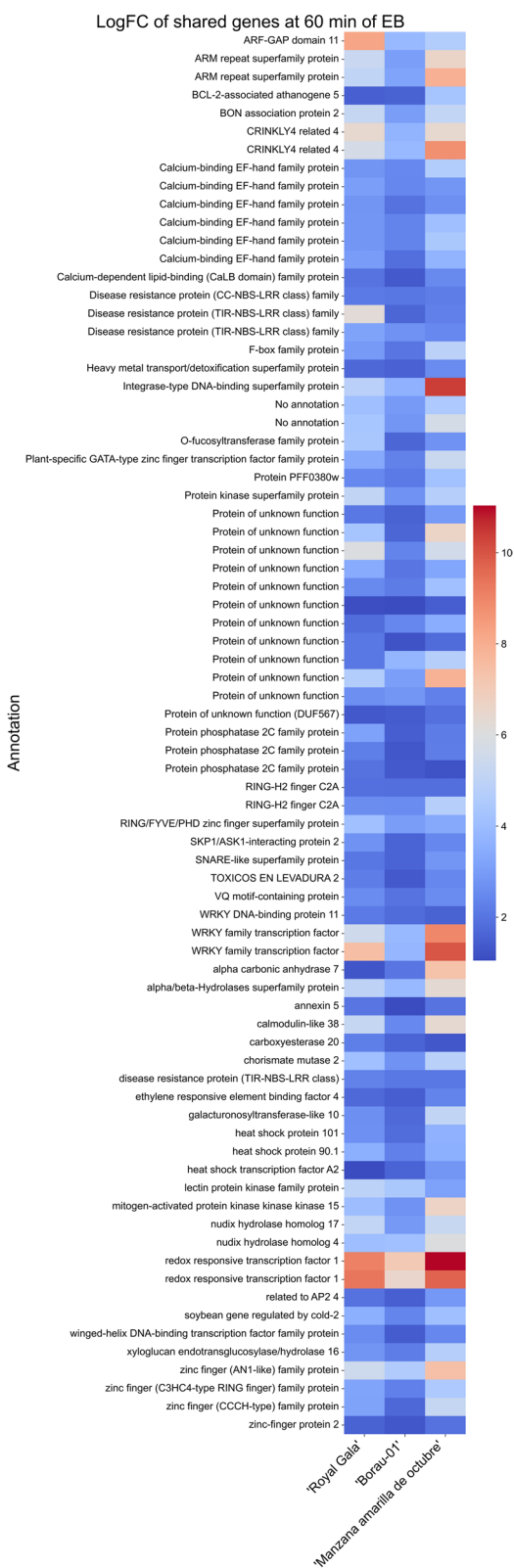


Fig. 3 Heatmap of shared DEGs among all cultivars at 60 min. Expression changes are shown as $|\log_2FC|$ values, greater values are coloured in red

Weighed gene co-expression network analysis reveals highly conserved domain in gene cluster related to enzymatic browning

WGCNA allows interpretation of RNA-seq data to find clusters of genes co-expressed that can also be correlated with a trait [43]. After logCPM data filtration, 33,661 expressed genes were analysed for WGCNA. PCA analysis of gene expression values for each sample was performed and showed a clear segregation of groups of samples into genotype clusters in PCA axis (Figure S3). Stranded mRNA data were analysed in a TOM matrix and clustered into 13 different gene modules (Table 3, table S5, Figure S4).

Analysis of gene modules correlation to different enzymatic browning indexes revealed a significant relationship between module Magenta and EB. Modules Magenta, Salmon and Cyan were significantly correlated ($p < 0.05$) to normalized CIE colour difference (ΔE^*) and difference in BI (ΔBI) from the time of cutting, whereas Magenta was also correlated to CIEDE2000 colour difference (ΔE_{00}) and browning index (BI) (Fig. 6). Both the number of genes (Table 3) and gene expression patterns (Figure S4) associated to each module pointed out that neither Salmon nor Cyan modules are relevant to enzymatic browning response, and a strong correlation between phenotype and expression changes was found in module Magenta. A Gene Ontology enrichment analysis of Magenta module genes revealed several enriched terms in all categories also found in differential expression analysis (Fig. 7). This analysis suggested a common pool of genes involved in several metabolic processes also present in ‘high and low browning genotypes’ DEGs at 60 vs 0 min. Transcription regulation is heavily represented by several enriched terms such as ‘binding’ (GO:0005488), ‘DNA-binding transcription factor activity’ (GO:0003700), ‘transcription factor regulator activity’ (GO:0140110), etc. Posttranslational modification and protein degradation processes can also be found among terms such as ‘protein serine/threonine phosphatase activity’ (GO:0004722), ‘protein phosphorylation’ (GO:0006468), ‘ubiquitin-protein transferase activity’ (GO:0004842) and ‘protein modification process’ (GO:0036211). Biological Process and Cell Component enriched terms also coincide with those found previously in DEGs analysis revealing involvement of response to stress genes and different cellular components participation in cell defence responses (Fig. 7). These results suggest an intricate network of molecular mechanisms involved in response to enzymatic browning. Identifying a common regulator could lead to new tools for controlling enzymatic browning and similar stresses in apples.

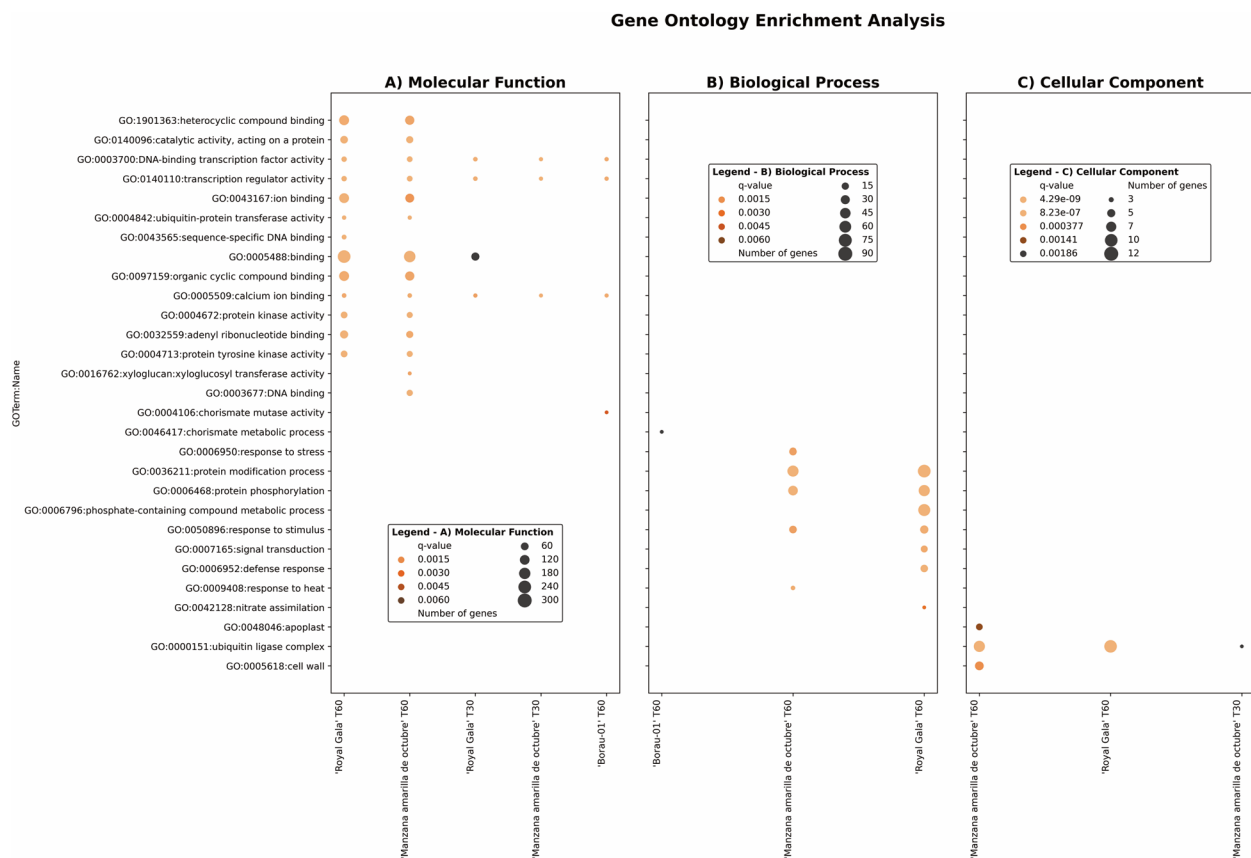


Fig. 4 GO Enrichment graphical representation of enriched terms obtained with Benjamin-Hochberg's test from the 412 unique (51.56%) DEGs. GO enrichment categories from top to bottom: **A)** Molecular Function, **B)** Biological Process and **C)** Cellular Component. Samples are shown in x axis whereas enriched terms in y axis. Bigger size of dots equals a higher number of genes related with enriched terms. A lighter colour means a more significant p -value

Calcium binding cis-regulatory elements co-regulate enzymatic browning

To identify such regulators, we conducted a peak-motif analysis of the upstream sequences of magenta module genes. Analysis of *cis*-regulatory elements was conducted on Magenta gene module selecting 4 upstream regions with different lengths. Regions from -1500 to $+200$ (TSS), -500 to $+200$, -500 to 0 and from 0 to $+200$ were evaluated and discovered motifs were scanned using curated databases to find similar motifs and binding transcription factors. After evaluation of retrieved motifs from RSAT (Regulatory Sequence Analysis Tools) analysis, upstream region 4 (from 0 to $+200$) was discarded and we obtained a list of 15 binding motifs from upstream region 1, 2 and 3 (Table 4). Motifs from these three upstream regions were slightly different from one to another but some of them matched with identical transcription factor binding sites. These transcription factors' binding sites belonged to several TFs families, including Calmodulin-Binding Transcription Activators (CAMTA), WUSCHEL and WRKY.

All discovered motifs (Table 4) showed a normalized correlation with matching database motifs between 0.459 and 0.817 and kmers ranging from 78.62 to 87.33 . All found motifs showed a conserved 'GCGC' box that displayed great heterogeneity at both upstream and downstream sides, pointing out the complex regulation among co-expressed genes during enzymatic browning. The degenerate code of motifs discovered showed that different variations of nucleotides are present in Magenta gene cluster. We identified 33 transcription factors (TFs) (Fig. 8, Table S6) in the Magenta gene cluster, belonging to various families such as heat transcription factors (MD14G1015900), WRKY (MD06G1104100), ERF (MD10G1094700), and GRAS (MD11G1229600). Although these TFs did not exhibit a significant change in expression in all cases, we identified four whose expression changed significantly at 30 and 60 min in all cultivars, with expression levels notably higher than those of the other TFs. These four transcripts corresponded to an integrase-type DNA-binding superfamily protein (MD15G1221100), a redox-responsive transcription

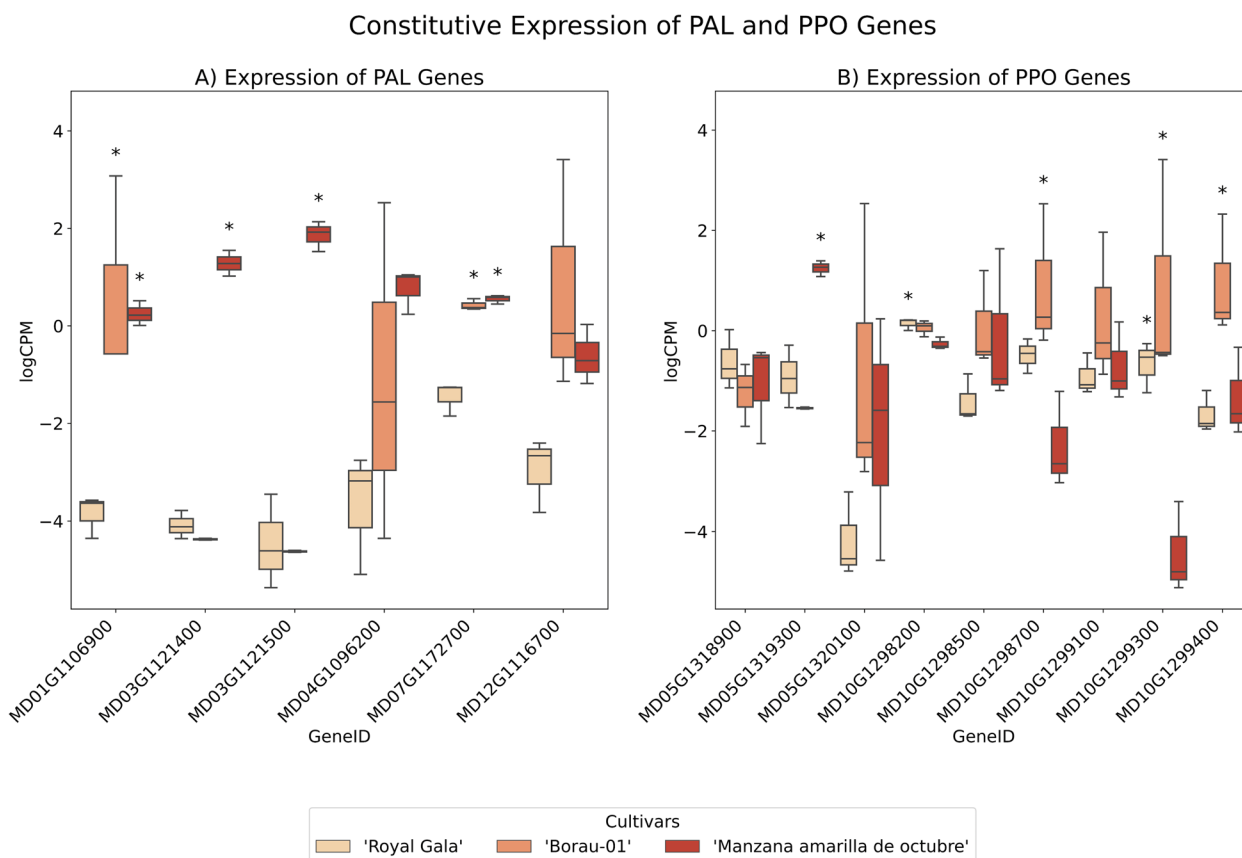


Fig. 5 **A** logCPM expression values of PAL genes at T0 in all cultivars. **B** logCPM expression values of PPO genes at T0 in all cultivars. Significant differences are marked as * according to Tukey test ($p < 0.05$)

Table 3 Number of genes of gene modules found in WGCNA (Weighted gene co-expression network analysis)

Module color	Number of genes
Black	487
Blue	5946
Brown	3432
Cyan	3275
Green	222
Greenyellow	55
Magenta	323
Pink	1725
Purple	2033
Red	7025
Salmon	7239
Tan	84
Turquoise	1815

factor 1 (MD05G1080900), and two WRKY family transcription factors (MD06G1104100, MD14G1123000), which we consider to be of great interest for future browning related studies.

Discussion

Enzymatic browning has been extensively investigated from different approaches as a fruit affection leading to economic and organoleptic properties losses in apple affecting colour (Fig. 1), flavour and nutritional properties [13, 49, 50]. However, the regulatory mechanisms underlying EB and effective control strategies remain poorly understood. Therefore, this study explores the molecular mechanisms of EB and its coordination by comparing low-browning ('Royal Gala'), intermediate-browning (Borau- 01) and high-browning ('Manzana amarilla de octubre') apple genotypes. The results highlight the interplay of cell wall restructuring, redox homeostasis, and transcription factor regulation in EB responses with a total of 1448 DEGs in the three apple genotypes during fresh cutting (0, 30 and 60 min) (Fig. 2). Notably, there were more up-regulated DEGs than

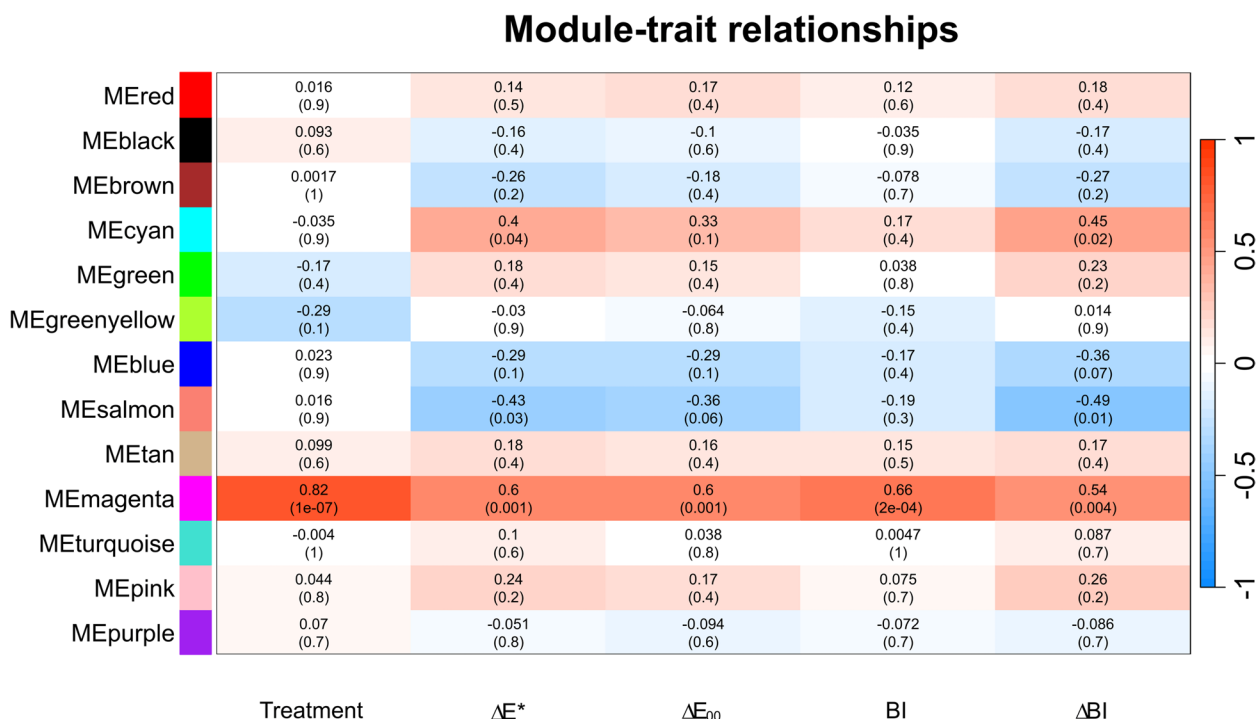


Fig. 6 Correlation values of gene modules with Time (treatment) and several enzymatic browning indexes (ΔE^* , ΔE_{00} , BI, ΔBI). Modules are shown at left side coloured by name. Positive correlation values are shown in red, whereas negative values are represented in blue. Each correlation value is followed by its *p*-value

down-regulated DEGs in the browning process (Fig. 2, Table S3), in accordance with other studies [6, 16, 49].

Transcriptome changes during EB result in the reparation of physical cell barriers and regulation of energy metabolism

Several studies have reported notable changes in expression of genes related to secondary metabolism, lipid metabolism and cell wall modification in relation to enzymatic browning after processing [6, 10, 17]. In this study, shared transcriptomic responses in the three genotypes included upregulation of genes involved in cell wall restructuring (e.g., pectin methylesterase inhibitors, xyloglucan endotransglucosylase) and vesicle trafficking (e.g., exocyst subunits) (Fig. 2B, Fig. 3; Fig. 9). Among these group of genes, ‘Royal Gala’ and ‘Manzana amarilla de octubre’ shared the highest number of genes (Fig. 2), which include ‘exocyst subunit exo70’ (MD12G1133300, MD11G1116300) (Table S3, Fig. 3), known to be involved in vesicle trafficking and responsible of thickening of cell walls during pathogenesis [51–53], several ‘plant invertase/pectin methylesterase inhibitor superfamily proteins’ (MD03G1290900, MD11G1307600) and ‘xyloglucan endotransglucosylase/hydrolases’ (MD09G1152600, MD13G1268900, MD16G1267200) which are directly responsible for cell wall reorganization through pectin transformation and further signalling [54, 55]. Furthermore,

several WAK and MAPK genes, known to be correlated in a pectin-initiated signal pathway [56], are highly up-regulated in both cultivars (Fig. 3, Fig. 9) and has also been reported to be up-regulated in a similar recent study in *Malus domestica* [57]. In addition, lipid membranes reorganize significantly during cellular stress. At 60 min after oxidation, several lipid metabolism-related DEGs were up-regulated (Table S2), including ‘alpha/beta hydrolase’ genes, which were also involved in membrane integrity in previous studies [6], a ‘phosphoglycerate mutase’ and a ‘3-ketoacyl-coA synthase 11’, a gene proposed to promote wax formation [58]. Additionally, a ‘diacylglycerol kinase 5’ and a ‘fatty acid desaturase’ were up-regulated, both of which are related to phospholipid synthesis and the scavenging of toxic intermediates during membrane reorganization [12, 58]. Highly expressed ‘lipoxygenases’ genes in ‘Royal Gala’ and ‘Manzana amarilla de octubre’ might be essential for jasmonic acid synthesis, regulated by overexpressed ‘CRINKLY 4’ transcription factors (MD08G1217500, MD15G1404800) (Table S2, Fig. 3), suggesting that this family of transcription factors plays a key role in the regulation of lipid metabolism and hormone signalling [59]. This is also supported by the overexpression of a ‘carboxysterase 20’ (MD00G1003500) in all 3 genotypes (Fig. 3), which has been shown to participate in these processes [60].

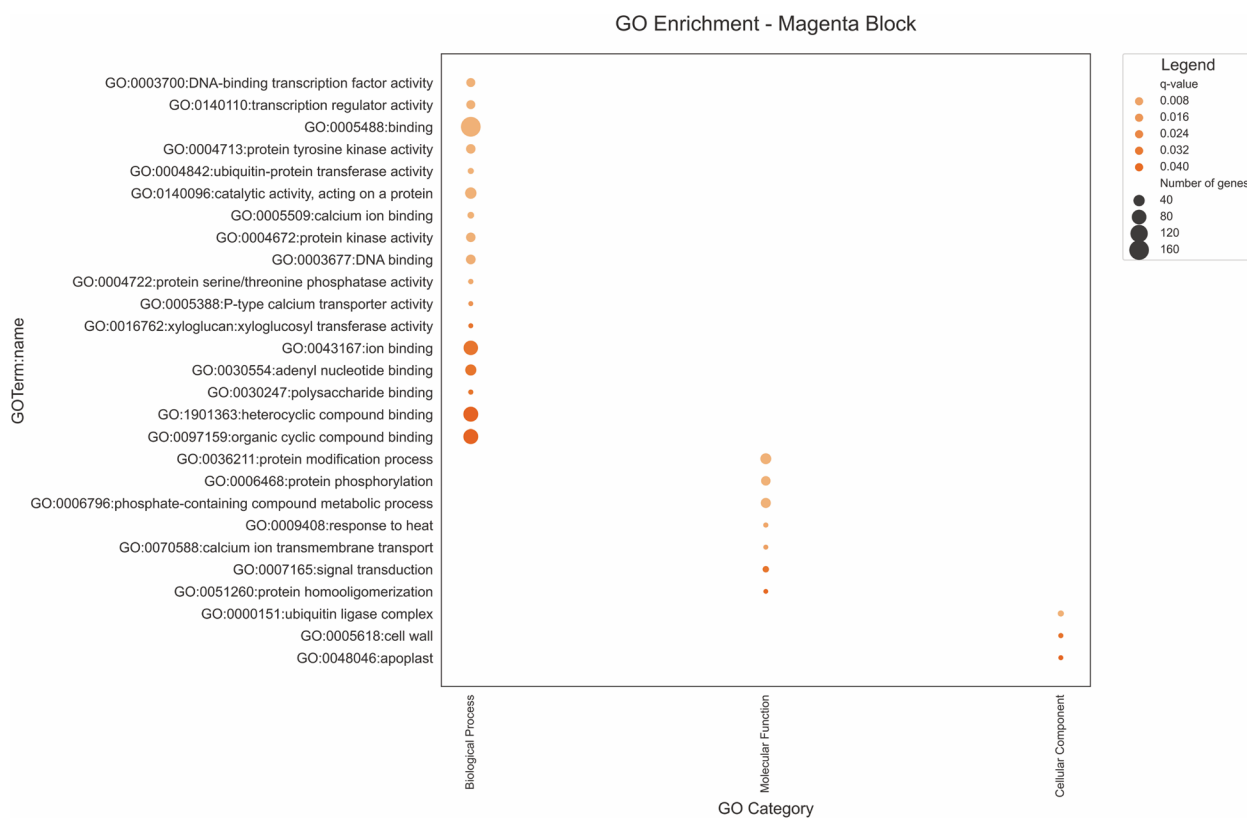


Fig. 7 GO Enrichment analysis of Magenta module genes (323 genes). X axis represents GO category whereas Y axis shows enriched terms. Significance is shown with colour gradient and number of genes covered by each term is represented with dot size

On the other hand, protein degradation was significantly up-regulated in all cultivars at T60, with several gene families including 7 plant U-box genes in Magenta WGCNA cluster and several ARM repeat superfamily protein genes (Table 2, Table S6) [61]. Furthermore, the overexpression of two ‘Ribosome inactivating protein bryodin II’ (MD06G1085500) and ‘DegP protease 9’ (MD17G1038400), 3 genes related to vesicle trafficking (an ‘annexin 5’ (MD15G1372900), an ‘ARF-GAP domain 11’ (MD10G1150400), and a ‘SNARE-like superfamily protein’ (MD05G1005900) suggested proteome reorganization during EB (Fig. 3, Table S3).

Furthermore, energy metabolism was also impacted during enzymatic browning to meet metabolic demands, with modest ATPase expression increases except for highly overexpressed calcium ATPase 2 genes (MD15G1296400) in ‘Royal Gala’ and ‘Manzana amarilla de octubre’ at T60 and a calcium ATPase2 (MD02G11850) only overexpressed in ‘Royal Gala’. Finally, secondary metabolism was also influenced, showing a ‘chorismate mutase 2’ gene (MD15G1040000), which is involved in phenolic compound biosynthesis, highly overexpressed in all cultivars at T60, consistent with observations by Mellidou et al. [6].

Regarding *genotype-specific mechanisms*, ‘Royal Gala’ exhibited unique upregulation of genes linked

to microfibril reorganization and stress signalling, a ‘COBRA-like protein precursor’ (MD17G10642), involved in microfibril reorganization [62, 63], and a syntaxin of plants 121 (MD14G10410) (Table S3). High-browning genotype showed increased expression of actin cross-linking proteins and expansins, emphasizing structural reorganization (Table S3), such as ‘actin cross-linking protein’ (MD16G10808) and an ‘expansin A4’ (MD04G11298). Additionally, ‘Royal Gala’ also overexpressed a ‘chalcone-flavanone isomerase family protein’ (MD08G10729) (Table S3). Apart from the phenylpropanoid biosynthesis pathway, other minor metabolic pathways and transport proteins were also up-regulated, including a ‘nitrate transporter’ in ‘Royal Gala’ at T60, which could enhance glutathione synthesis. Overall, enzymatic browning triggers a dynamic response in all studied cultivars, covering key metabolic processes to ensure wound healing and homeostasis balance, with gene expression patterns varying by genotype.

Enzymatic browning response triggers changes in redox homeostasis-related genes and other metabolic pathways

The browning of fruits and vegetables is closely related to ROS metabolism in plants [7, 10]. In our study, several

Table 4 15 binding motifs found in WGCNA magenta module and their corresponding best matches. Motif discovery results of 3 upstream regions of Magenta WGCNA gene module

Upstream Region	Region start	Region end	Motif	Sequence	kmer	evalue	Ncor	Accession name	Names	Binding TFs
3	- 500	0	4	raaaaCGCGTtgd	87.33	4.70E- 88	0.817	MA1197.1 (JASPAR 2024), M0350 (Ath- alianaCistrome v4_May2016)	CAMTA1, CAMTA1.DAP, T27097;	Q9 FY74 (Ankyrin repeat, IQ calmodulin-binding motif, CG- 1 domain, Ankyrin repeats (3 copies)) T27097 (Ankyrin repeat, IQ calmodulin-binding motif, CG- 1 domain, Ankyrin repeats (3 copies)) Q9 FY74
3	- 500	0	5	rkaaaCGCGTcskb	87.33	4.70E- 88	0.778	UN0362.1 (JASPAR 2024)	EICBP-B, EICBPB	F4 KCL4 (Ankyrin repeat, IQ calmodulin-binding motif, CG- 1 domain, Ankyrin repeats (3 copies)) Q9 FY74
3	- 500	0	1	rdaaaCGCGTtkdk	87.33	4.70E- 88	0.748	UN0362.1 (JASPAR 2024)	EICBP-B, EICBPB	F4 KCL4 (Ankyrin repeat, IQ calmodulin-binding motif, CG- 1 domain, Ankyrin repeats (3 copies)) F4 KCL4 (Ankyrin repeat, IQ calmodulin-binding motif, CG- 1 domain, Ankyrin repeats (3 copies))

Table 4 (continued)

Upstream Region	Region start	Region end	Motif	Sequence	kmer	evalue	Ncor	Accession name	Names	Binding TFs
3	- 500	0	2	kkaaACGGGtbks	87.33	4.70E- 88	0.731	MA1197.1 (JASPAR 2024), M0350 (Ath- alianaCistrome v4_May2016)	CAMTA1, CAMTA1.DAP, T27097;	Q9 FY74 (Ankyrin repeat, IQ calmodulin-binding motif, CG- 1 domain, Ankyrin repeats (3 copies)) T27097 (Ankyrin repeat, IQ calmodulin-binding motif, CG- 1 domain, Ankyrin repeats (3 copies)) Q9 FY74
3	- 500	0	3	sgcystctccs-caCaCGGtttky	87.33	4.70E- 88	0.492	UN0362.1 (JASPAR 2024)	EICBP-B, EICBPB	F4 KCL4 (Ankyrin repeat, IQ calmodulin-binding motif, CG- 1 domain, Ankyrin repeats (3 copies)) Q9 FY74
2	- 500	200	1	rsacACCGTGtggk	86.04	9.10E- 87	0.732	UN0362.1 (JASPAR 2024)	EICBP-B, EICBPB	F4 KCL4 (Ankyrin repeat, IQ calmodulin-binding motif, CG- 1 domain, Ankyrin repeats (3 copies))

Table 4 (continued)

Upstream Region	Region start	Region end	Motif	Sequence	kmer	evalue	Ncor	Accession name	Names	Binding TFs
2	- 500	200	5	rmaCAGCGGC GTGtky	86.04	9.10E- 87	0.654	MA1382.1 (JASPAR 2024), M0371 (Ath- alianaCistrome v4_May2016)	FAR1, FAR1. DAP, T17156;	Q9SWG3/ T17156 (FAR1 DNA-binding domain, SWIM zinc finger, MULE transposase domain) Q9SWG3
2	- 500	200	5	rmaCAGCGGC GTGtky	86.04	9.10E- 87	0.6	UN0362.1 (JASPAR 2024)	EICBP-B, EICBPB	F4 KCL4 (Ankyrin repeat, IQ calmodulin-binding motif, CG- 1 domain, Ankyrin repeats (3 copies))
2	- 500	200	3	sggcGGcGkcGGa- raCGCtGkGk	86.04	9.10E- 87	0.594	M0351 (Ath- alianaCistrome v4_May2016)	CAMTA5, DAP, T18903;	T18903 (Ankyrin repeat, IQ calmodulin-binding motif, CG- 1 domain, Ankyrin repeats (3 copies), Ankyrin repeat, Ankyrin repeats (many copies))
2	- 500	200	4	sbssyctctctccc- cACGCGTgttb	86.04	9.10E- 87	0.459	UN0362.1 (JASPAR 2024)	EICBP-B, EICBPB	F4 KCL4 (Ankyrin repeat, IQ calmodulin-binding motif, CG- 1 domain, Ankyrin repeats (3 copies), Ankyrin repeat, Ankyrin repeats (many copies))
2	- 500	200	2	sscbrcctcgrrccGCC GCCtGkcb	86.04	9.10E- 87	NO MATCH	NO MATCH	NO MATCH	NO MATCH

Table 4 (continued)

Upstream Region	Region start	Region end	Motif	Sequence	kmer	evalue	Ncor	Accession name	Names	Binding TFs
1	- 1500	200	3	rmaaACGCGTtagd	78.62	2.40E- 79	0.804	MA1197.1 (JASPAR 2024), M0350 (Ath- alianaCistrome v4_May2016)	CAMTA1, CAMTA1.DAP, T27097;	Q9 FY74 (Ankyrin repeat, IQ calmodulin-binding motif, CG- 1 domain, Ankyrin repeats (3 copies)) T27097 (Ankyrin repeat, IQ calmodulin-binding motif, CG- 1 domain, Ankyrin repeats (3 copies)) Q9 FY74
1	- 1500	200	5	cvcacACGCGTttkb	78.62	2.40E- 79	0.754	UN0362.1 (JASPAR 2024)	EICBP-B, EICBPB	F4 KCL4 (Ankyrin repeat, IQ calmodulin-binding motif, CG- 1 domain, Ankyrin repeats (3 copies)) Q9 FY74
1	- 1500	200	1	raaaACGCGTttkb	78.62	2.40E- 79	0.747	UN0362.1 (JASPAR 2024)	EICBP-B, EICBPB	F4 KCL4 (Ankyrin repeat, IQ calmodulin-binding motif, CG- 1 domain, Ankyrin repeats (3 copies))

Table 4 (continued)

Upstream Region	Region start	Region end	Motif	Sequence	kmer	evalue	Ncor	Accession name	Names	Binding TFs
1	- 1500	200	2	ssaaACGCGGtsks	78.62	2.40E- 79	0.712	MA1197.1 (JASPAR 2024), M0350 (Ath-alianaCistrome v4_May2016)	CAMTA1, CAMTA1.DAP, T27097;	Q9FY74 (Ankyrin repeat, IQ binding motif, CG- 1 domain, Ankyrin repeats (3 copies)) T27097 (Ankyrin repeat, IQ binding motif, CG- 1 domain, Ankyrin repeats (3 copies)) Q9FY74
1	- 1500	200	5	cvcacACGCGTttkb	78.62	2.40E- 79	0.712	MA1382.1 (JASPAR 2024), M0371 (Ath-alianaCistrome v4_May2016)	FAR1, FAR1.DAP, T17156;	Q9SWG3/ T17156 (FAR1 DNA-binding domain, SWIM zinc finger, MULE transposase domain) Q9SWG3
1	- 1500	200	1	raaaACGCGTttkb	78.62	2.40E- 79	0.61	6ryL_DE (3D-foot-print 20,231,221)	Protein WUSCHEL	6ryL_E (Homeobox domain) 6ryL_D (Homeobox domain)
1	- 1500	200	2	ssaaACGCGGtsks	78.62	2.40E- 79	0.608	M0582_1.02 (CISBP 1.02)	AT5G64220, T071557_1.02	T071557_1.02 (Ankyrin repeat, IQ binding motif, CG- 1 domain, Ankyrin repeats (3 copies), Ankyrin repeat)

Table 4 (continued)

Upstream Region	Region start	Region end	Motif	Sequence	kmer	evalue	Ncor	Accession name	Names	Binding TFs
1	- 1500	200	3	rmaaACGCGTagd	78.62	2.40E- 79	0.599	M0581_1.02 (CISBP 1.02)	CAMTA3, T071553_1.02	T071553_1.02 (Ankyrin repeat, IQ calmodulin-binding motif, CG- 1 domain, Ankyrin repeats (3 copies))
1	- 1500	200	4	rba-maCGCGtCvrsG-CGCGttbb	78.62	2.40E- 79	0.574	M0351 (Ath-alianaCistrome v4_May2016)	CAMTA5.DAP, T18903;	T18903 (Ankyrin repeat, IQ calmodulin-binding motif, CG- 1 domain, Ankyrin repeats (3 copies), Ankyrin repeat, Ankyrin repeats (many copies))

Certain motif can have more than one matching TF as a selection of best Ncor entires was made. From left to right: Upstream region (name of sequence length selected during RSAT analysis); region start; region end, motif number, motif sequence, kmer (motif scoring value), evalue, Ncor (normalized correlation with databases motifs), Accession name of matching motif, names of matching motifs, matching motifs' binding TFs. Motif nucleotides are annotated following Nucleotide base codes (IUPAC)

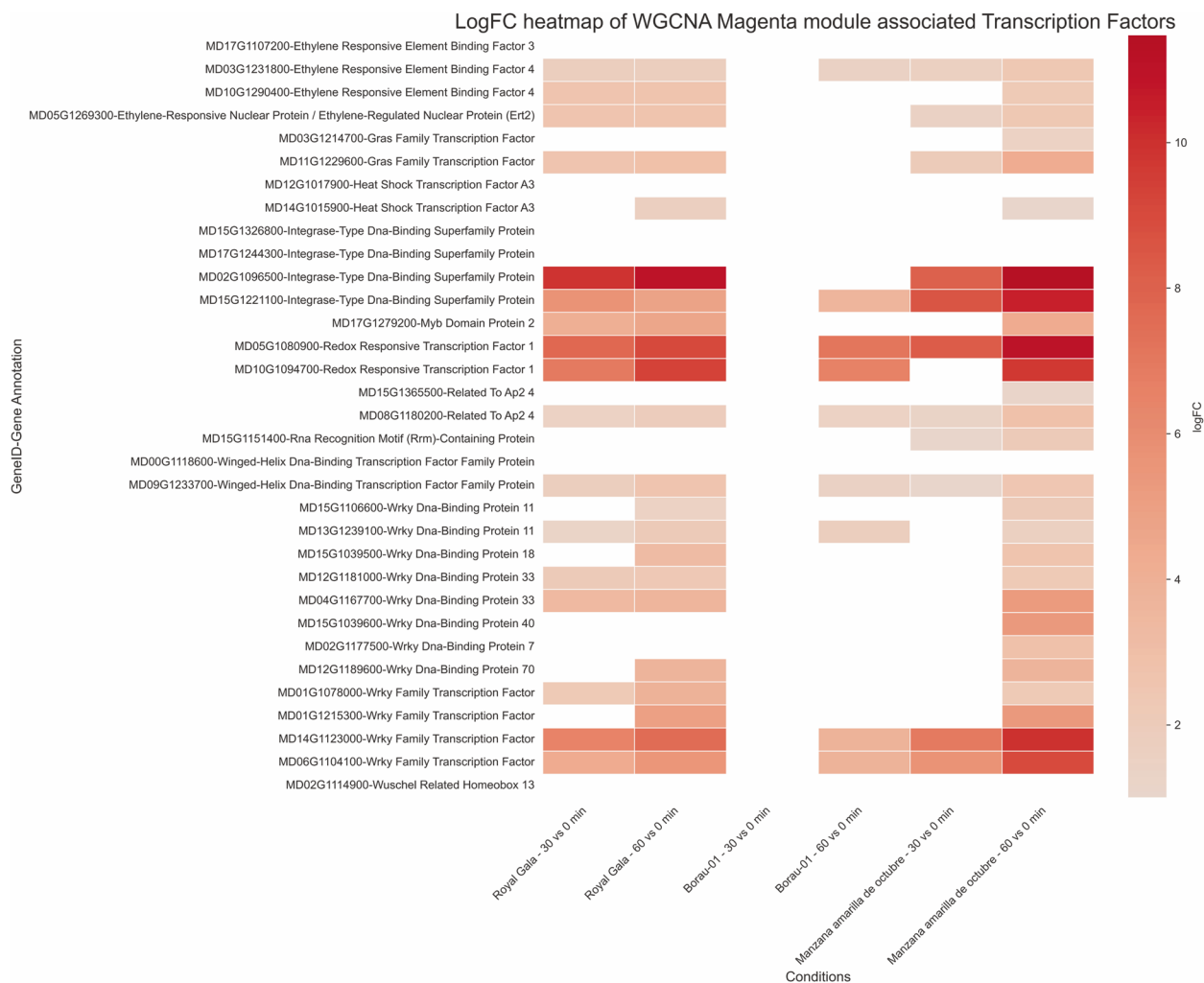


Fig. 8 Expression changes of 33 annotated transcription factors (TFs) found in WGCNA Magenta gene module. Expression is shown as $|\log_2FC|$ values between different oxidation times across all studied cultivars (30 min vs 0 min and 60 min vs 0 min)

ROS-related DEGs were identified (Table S3), indicating both common and cultivar-specific responses to EB (Fig. 3, Table S3), with variations in gene expression potentially contributing to enhanced stress tolerance.

Redox homeostasis genes exhibit genotype-specific expression, with shared differential expression of detoxifying enzymes across cultivars at 60 min of oxidation, like Cytochrome P450, previously predicted to be involved in EB [64] and nudix hydrolases, extensively involved in biotic and abiotic stress responses in different plant species and potentially regulating basal immunity through different pathways (table S3, Fig. 3) [65]. Among well-known antioxidant enzymes catalases (*CAT*) and superoxide dismutases (*SOD*), only catalase genes were differentially expressed in the three studied cultivars, contrasting with previous studies on activity changes of these enzymes during EB (Table S3) [9, 12, 15]. However, this lack of transcriptional regulation

does not rule out changes in enzyme activity or post-translational modifications, which could be modulated through other regulatory mechanisms. As a cycle was also regulated during EB and, although a clear pattern of expression for *APX*, *DHAR* and *MDHAR* was not detected in our cultivars (Figure S2) as previously done by Mellidou, a 'nucleobase-ascorbate transporter 12' gene (MD03G1135100) was up-regulated in 'Royal Gala' at T60 vsT0, suggesting a rebalance of this cycle that could make this genotype more efficient leading with reactive oxygen species. Finally, a glutamine-dumper 3 (MD13G1263000) and a common Pyridoxal phosphate (PLP)-dependent transferases superfamily protein (MD00G1005100), which plays an important role in Vitamin B synthesis and crucial for UV damage protection [66], were found for the first time in shared DEGs (Fig. 3), suggesting a diversified response to EB. Therefore, a conserved response remains as shown by 8 shared DEGs

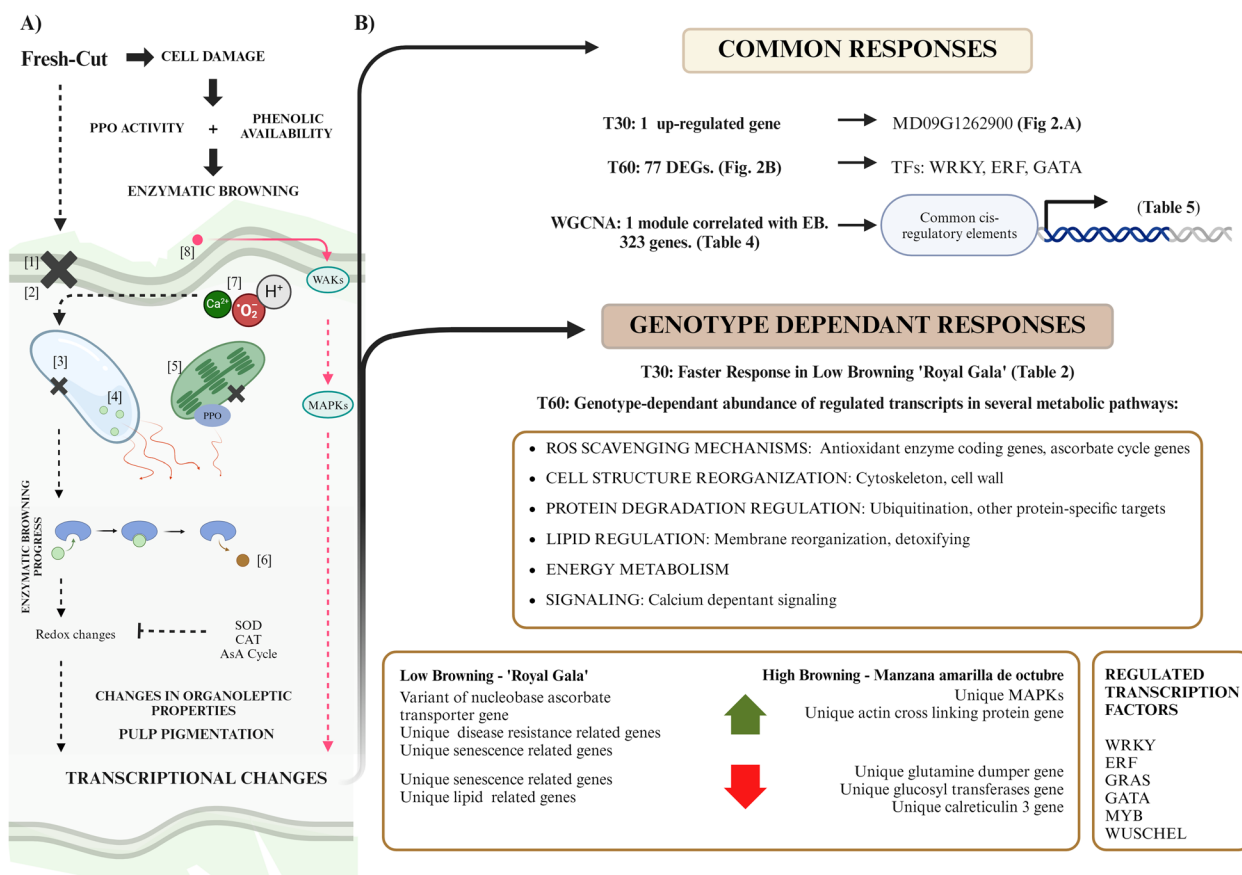


Fig. 9 **A** General schematic view of enzymatic browning (EB) in apple pulp and proposed pectin-related signaling pathway. 1: Cell wall. 2: Cell membrane. 3: Vacuole 4: Phenolic compounds. 5: Chloroplast. 6: Enzymatic browning reaction catalyzed by PPO and resulting in Melanin formation. 7: Ion availability. **B** Main findings on transcriptome changes among studied cultivars. Shared and specific responses are shown with special emphasis on affected metabolic pathways and regulatory elements

(MD06G1232000, MD14G1238600, MD01G1209100, MD01G1209200, MD08G1124700, MD15G1104100, MD11G1039300, MD13G1116400, MD13G1112700) in Magenta WGCNA cluster that belong to previously mentioned gene families (Table S5).

Identification and diversity of overexpressed transcription factors (TF) in response to enzymatic browning

Several TFs genes (e.g., MYB, WRKY, bHLH, Ex NAC, ERF, bZIP and HSF) were reported to be differentially expressed during plant stress responses [67]. However, to our knowledge, few studies have identified TFs among the DEGs related to the browning process of freshly cut apples [16]. In this work, the analysis of cis-regulatory elements in a co-expressed gene cluster correlated to enzymatic browning allowed the identification of several binding motifs. These motifs, with degenerate code between genes, can accommodate the binding of different TF isoforms from WRKY, WUSCHEL and CAMTA families (Table 4). Moreover, analysis of intramodular

connectivity of WGCNA Magenta cluster genes allowed identification of a pool of genes whose interactions in the network have a theoretical higher weight, indicating either more numerous or stronger interactions (Table 5). These identified genes belong to ERF (8 genes), WRKY (12 genes), calcium binding EF-hand families (9 genes) (Table S5, Fig. 8), as well as other genes whose orthologs have been linked to pathologies [68–71]. The higher ERF and WRKY transcription factor expression patterns observed in the current study was consistent with a previous study on browning in freshly cut potato and apple [16, 28]. These findings, along with severe overexpression of ‘calmodulin-like 38’ genes and ‘ethylene redox responsive transcription factor 1’ genes in all cultivars at T60 (Table S3, Table S5), suggest a complex interplay between transcription factor families and downstream effectors. This interaction likely involved both positive and negative feedback loops, strongly influenced by Ca²⁺ signalling, as a great number of these calcium-dependant genes have been found in all samples both in common and specific

Table 5 Top 20 genes with highest intramodular connectivity of Magenta module after WGCNA

Gene ID	Function	GS.BI	p.GS.BI	kWithin
MD02G1096500	Integrase-type DNA-binding superfamily protein	0.76	4.87E- 06	14.73
MD12G1216300	soybean gene regulated by cold- 2	0.7	4.86E- 05	14.51
MD03G1087100	zinc finger (C3HC4-type RING finger) family protein	0.76	4.88E- 06	14.15
MD09G1152600	xyloglucan endotransglucosylase/hydrolase 16	0.64	2.91E- 04	13.57
MD14G1123000	WRKY family transcription factor	0.81	3.56E- 07	13.48
MD05G1005900	SNARE-like superfamily protein	0.66	1.66E- 04	13.06
MD16G1164700	TOXICOS EN LEVADURA 2	0.66	1.68E- 04	12.81
MD13G1028700	Protein of unknown function	0.71	3.22E- 05	11.95
MD02G1178100	SKP1/ASK1-interacting protein 2	0.64	2.95E- 04	11.85
MD03G1297400	Protein of unknown function	0.69	6.72E- 05	11.71
MD03G1185700	Calcium-binding EF-hand family protein	0.68	9.20E- 05	11.49
MD10G1102000	Protein phosphatase 2C family protein	0.54	3.43E- 03	11.44
MD09G1039300	zinc finger (AN1-like) family protein	0.79	1.22E- 06	11.35
MD04G1167700	WRKY DNA-binding protein 33	0.71	3.74E- 05	10.95
MD05G1080900	redox responsive transcription factor 1	0.86	6.66E- 09	10.93
MD06G1104100	WRKY family transcription factor	0.75	7.18E- 06	10.8
MD17G1244500	Protein of unknown function	0.6	9.57E- 04	10.78
MD11G1229600	GRAS family transcription factor	0.57	1.82E- 03	10.61
MD04G1202100	Protein PFF0380w	0.59	1.10E- 03	10.42
MD05G1325400	F-box family protein	0.71	3.75E- 05	10.2

From left to right: GeneID; Function; GS.BI: Correlation between gene and Browning index; p.GS.BI: p-value of GS.BI; kWithin: Intramodular connectivity value

responses (Table S2, Table S4). However, the activation mechanisms and sequence of action of these transcription factors remain poorly understood. Furthermore, the enzymatic browning response of *Malus domestica* also triggers overexpression of many disease-resistance, heat response and stress-related genes, which are also part of enriched terms in the GO Ontology analysis (Fig. 7, Table 6). One of such genes, MD01G1148800, was overexpressed in response to fire blight in *Malus domestica* roots [72], whereas other overexpressed genes in our assay such as lipoxygenases, cupredoxins, *WRKY*, *ERF* and *CAMTA* genes have also been related to other pathologies [70, 71, 73–75]. Therefore, as plants lack an adaptative immune system, the tissue breakdown induced by mechanical damages due to abiotic factors might be similar to that caused by insect herbivory or microbial infection. Hence, it is not surprising that the DEGs associated with browning were mainly related to the interaction between plants and pathogenic microorganisms. Furthermore, these interactions are influenced by ion binding specificity and rely on ion concentrations such as Ca^{2+} or Zn^{2+} . This study establishes a foundation for further function studies of several transcription factor families (*WRKY*, *ERF*, *GRAS*, *GATA*, *WUSCHEL*, *CAMTA*) as probable candidates for fresh cut browning responses.

Conclusions

Transcriptomic changes have been observed in three apple cultivars with different enzymatic browning phenotypes over time after fresh cutting (0, 30 and 60 min). The most significant transcriptomic events were detected in all cultivars 60 min after cutting, providing a transcriptome database and candidates genes for future molecular studies of enzymatic browning. Detailed comparison of DEGs between cultivars, as well as the identification of genes clustered in relation to EB, revealed a common response to EB shared by all genotypes. This response involves critical cellular processes including vesicle trafficking, cytoskeleton reorganization, lipid metabolism (crucial for energetic production and structural integrity), secondary metabolism, protein degradation and transcription regulation. The gene pool associated with the conserved response of apple pulp to EB at 60 min includes a diverse set of DEGs encoding calcium-binding proteins, heat shock proteins, redox-responsive transcription factors, *WRKY* transcription factors, zinc finger proteins, and disease resistance proteins, among other. Furthermore, *specific genotype responses* in nitrate and glutamine transport, redox homeostasis, cell restructuring and lipid metabolism among others were found between low and high browning genotypes, highlighting significant variations in constitutive expression of key enzymes such as PPO and PAL, confirming the complexity of this affection.

These findings provide valuable insights into the molecular mechanism involved in apple fresh-cut browning and offer new potential targets for EB regulation. However, more research is needed to validate the key DEGs and TFs identified in this study (eg. Knock out, RNA silencing or over-expression studies). The development of new technologies to disable candidate genes involved in EB offers the most promising strategy to avoid undesired browning in plant-derived products. This approach could enable the selection of apple genotypes enriched in beneficial phenolic compounds, while reducing the need for physical and chemical treatments in the food industry, therefore improving storability and reducing waste.

Abbreviations

BI	Browning Index
ΔBI	Difference in BI from the time of cutting
ΔE*	Normalized CIE colour difference from the time of cutting
ΔE00	CIEDE2000 colour difference from the time of cutting.
PPO	Polyphenol oxidase
PAL	Phenylalanine ammonia lyase
SOD	Superoxide dismutase
CAT	Catalase
APX	Ascorbate peroxidase
MDHAR	Monodehydroascorbate reductase
DHAR	Dehydroascorbate reductase
AsA	Ascorbic acid
WGCNA	Weighted Gene Co-Expression Network Analysis
DEGs	Differentially expressed genes
GO	Gene Ontology
CAMTA	Calmodulin binding transcription activator
ERF	Ethylene response factor
MAPK	Mitogen associated protein kinase
ARM	Armadillo
WAK	Wall Associated Kinase
TFBS	Transcription factor binding sites

Supplementary Information

The online version contains supplementary material available at <https://doi.org/10.1186/s12870-025-06445-6>.

Additional file 1: Table S1. Summary of Illumina sequencing data and mapped sequence reads for the assayed apple samples

Additional file 2: Table S2. Primer sequences of selected genes for qPCR validation of RNAseq data. GeneID, annotated name (based on GDDH13 Golden Delicious reference genome v1.1), given name, forward and reverse sequences, and amplicon length are provided for 8 DEGs and one housekeeping gene (WD-40)

Additional file 3: Table S3. Differentially expressed genes in 3 cultivars with different enzymatic browning susceptibility at 30 and 60 min of oxidation

Additional file 4: Table S4. GO Enrichment enriched terms summary

Additional file 5: Table S5. Gene expression in selected cultivars of WGCNA magenta module genes

Additional file 6: Table S6. Complete list of annotated transcription factors found at 30 and 60 min of oxidation between all apple cultivars. TFs and their corresponding expression level are shown for each cultivar and time comparison

Supplementary Material 7. Figure S1. A) Comparison of Log₂ FC expression values of 8 selected genes between RNAseq data and qRT-PCR at 60 min after cutting. Striped data correspond to RNAseq data whereas filled bars belong to qRT-PCR data. B) Linear expression values obtained by performing regression analysis between qRT-PCR and RNAseq data

Figure S2. Constitutive expression patterns of annotated genes belonging to genes of interest in studied cultivars at 0 min. Catalase- 2 genes are shown in blues. SOD genes (Fe superoxide dismutase 3, copper/zinc superoxide dismutase 1, copper/zinc superoxide dismutase 2, copper/zinc superoxide dismutase 3, manganese superoxide dismutase 1) are shown in reds. AsA cycle genes (ascorbate peroxidase 1, ascorbate peroxidase 3, ascorbate peroxidase 2, ascorbate peroxidase 4, ascorbate peroxidase 6, thylakoidal ascorbate peroxidase, monodehydroascorbate reductase 1, monodehydroascorbate reductase 4, monodehydroascorbate reductase 6, dehydroascorbate reductase, dehydroascorbate reductase 1, dehydroascorbate reductase 2) are shown in greens

Figure S3. PCA of logCPM gene expression values of sample replicates. Each sample's replicates colour is specified in the figure legend. 3 axis are represented. Each axis represents a component. The first three components explain 80% of observed variance among samples (PC1: 42%, PC2 35%, PC3: 3%)

Figure S4. Expression patterns of clustered genes in WGCNA modules. Each module's gene pool expression data was represented as logCPM values for all samples

Authors' contributions

AP, CM and PE conceptualized the study and acquired funding for the investigation. FJB, PI, PE and AP conducted field management. FJB, PI and AP conducted the laboratory RNA sample analysis. FJB and JG analyzed the transcriptomics data. CM, PI, FJB and PE performed the EB phenotyping. FJB and AP wrote the original manuscript. All authors contributed to the article and approved the final version of the manuscript.

Funding

This work has been funded by PID 2019 108081 RR Project (funded by MCIN/AEI 10.13039/501100011033 and the consolidated group A12 of Gobierno de Aragón – European social fund of the European Union).

Data availability

The raw reads generated during the current study have been deposited in Applecut Project with the accession number of PRJEB81442.

Declarations

Ethics approval and consent to participate

Not applicable.

Consent for publication

Not applicable.

Competing interests

The authors declare no competing interests.

Author details

¹Centro de Investigación y Tecnología Agroalimentaria de Aragón (CITA), Departamento de Ciencia Vegetal, Avenida Montañana 930, Zaragoza 50059, Spain. ²Instituto Agroalimentario de Aragón-IA2, CITA-Universidad de Zaragoza, Zaragoza 50013, Spain. ³UPNA, Dpto. Agronomía, Biotecnología y Alimentación, Campus de Arrosadía, Pamplona 31006, Spain. ⁴Instituto de Investigación Multidisciplinar en Biología Aplicada (IMAB), UPNA, Campus de Arrosadía, Pamplona 31006, Spain.

Received: 4 November 2024 Accepted: 24 March 2025

Published online: 12 April 2025

References

- FAOSTAT. Statistical Database. Rome: Food and Agriculture Organization of the United Nations; 2022. Accessed June 2024.
- Patocka J, Bhardwaj K, Klimova B, Nepovimova E, Wu Q, Landi M, et al. Malus domestica: A review on nutritional features, chemical composition, traditional and medicinal value. *Plants MDPI AG*. 2020;9:1–19.

3. Leri M, Scuto M, Ontario ML, Calabrese V, Calabrese EJ, Bucciantini M, et al. Healthy effects of plant polyphenols: Molecular mechanisms. *Int J Mol Sci*. MDPI AG. 2020;21(4):1250.
4. Rather RA, Bhagat M. Quercetin as an innovative therapeutic tool for cancer chemoprevention: Molecular mechanisms and implications in human health. Vol. 9, *Cancer Medicine*. United States: Blackwell Publishing Ltd; 2020. p. 9181–92.
5. Cofelice M, Lopez F, Cuomo F. Quality control of fresh-cut apples after coating application. *Foods*. 2019;8(6):189.
6. Mellidou I, Buts K, Hatoum D, Ho QT, Johnston JW, Watkins CB, et al. Transcriptomic events associated with internal browning of apple during postharvest storage. *BMC Plant Biol*. 2014;14(1):328.
7. Arnold M, Gramza-Michałowska A. Enzymatic browning in apple products and its inhibition treatments: A comprehensive review. Vol. 21, *Comprehensive Reviews in Food Science and Food Safety*. United States: John Wiley and Sons Inc; 2022. p. 5038–76.
8. Toivonen PMA, Brummell DA. Biochemical bases of appearance and texture changes in fresh-cut fruit and vegetables. *Postharvest Biol Technol*. 2008;48:1–14.
9. Wang X, Zhang X, Jia P, Luan H, Qi G, Li H, et al. Transcriptomics and metabolomics provide insight into the anti-browning mechanism of selenium in freshly cut apples. *Front Plant Sci*. 2023;14.
10. Singh B, Suri K, Shevkani K, Kaur A, Kaur A, Singh N. Enzymatic Browning of Fruit and Vegetables: A Review. In: *Enzymes in Food Technology*. Singapore: Springer Singapore; 2018. p. 63–78.
11. Ferreira Holderbaum D, Kon T, Kudo T, Pedro Guerra M. Enzymatic Browning, Polyphenol Oxidase Activity, and Polyphenols in Four Apple Cultivars: Dynamics during Fruit Development. *Hortsci*. 2010;45:1150–4.
12. Liu X, Zhang A, Zhao J, Shang J, Zhu Z, Wu X, et al. Transcriptome profiling reveals potential genes involved in browning of fresh-cut eggplant (*Solanum melongena* L.). *Sci Rep*. 2021;11(1):16081.
13. Fan J, Du W, Chen QL, Zhang JG, Yang XP, Hussain SB, et al. Comparative transcriptomic analyses provide insights into the enzymatic browning mechanism of fresh-cut sand pear fruit. *Horticulturae*. 2021;7(11):502.
14. Di Guardo M, Tadiello A, Farneti B, Lorenz G, Masuero D, Vrhovsek U, et al. A Multidisciplinary Approach Providing New Insight into Fruit Flesh Browning Physiology in Apple (*Malus domestica* Borkh.). *PLoS One*. 2013;8(10):e78004.
15. Tang T, Xie X, Ren X, Wang W, Tang X, Zhang J, et al. A difference of enzymatic browning unrelated to PPO from physiology, targeted metabolomics and gene expression analysis in Fuji apples. *Postharvest Biol Technol*. 2020;1:170.
16. Zuo W, Lu L, Su M, Zhang J, Li Y, Huang S, et al. Analysis of differentially expressed genes and differentially abundant metabolites associated with the browning of Meihong red-fleshed apple fruit. *Postharvest Biol Technol*. 2021;1:174.
17. Zhou H, Tian M, Huang W, Luo S, Hu H, Zhang Y, et al. Physiological and transcriptomic analysis of 'Whangkeumbae' pear core browning during low-temperature storage. *Gene Expr Patterns*. 2020;1:36.
18. Maioli A, Gianoglio S, Moglia A, Acquadro A, Valentino D, Milani AM, et al. Simultaneous CRISPR/Cas9 Editing of Three PPO Genes Reduces Fruit Flesh Browning in *Solanum melongena* L. *Front Plant Sci*. 2020;3:11.
19. R S, Rasane P, Singh A, Singh J, Kaur S, Nanda V, et al. Effect of herbal application on browning inhibition and physico-chemical quality of pear (*Pyrus communis*) slices. *South African J Botany*. 2024;165:505–16.
20. Chen C, Xie J, Gang J, Wang M, Wu K, Jiang A. Metabolomic insights into the browning inhibition of fresh-cut apple by hydrogen sulfide. *Food Chem*. 2024;447:139005.
21. Tazawa J, Oshino H, Kon T, Kasai S, Kudo T, Hatsuyama Y, et al. Genetic characterization of fresh browning trait in apple using the non-browning cultivar 'Aori 27'. *Tree Genet Genomes*. 2019;15(4):49.
22. Kunihiya M, Hayashi T, Hatsuyama Y, Fukasawa-Akada T, Uenishi H, Matsu-moto T, et al. Genome-wide association study for apple flesh browning: detection, validation, and physiological roles of QTLs. *Tree Genet Genomes*. 2021;17(11). Available from: <http://www.fao.org/faostat>.
23. Chi M, Bhagwat B, Lane WD, Tang G, Su Y, Sun R, et al. Reduced polyphenol oxidase gene expression and enzymatic browning in potato (*Solanum tuberosum* L.) with artificial microRNAs. *BMC Plant Biol*. 2014;14(1):62.
24. Xu K. Arctic Apples: A Look Back and Forward. *New York Fruit Quarterly*. 2015;23:21–4.
25. Wang T, Zhang C, Zhang H, Zhu H. CRISPR/Cas9-Mediated Gene Editing Revolutionizes the Improvement of Horticulture Food Crops. *J Agric Food Chem*. 2021;69(45):13260–9.
26. Chen Y, Lun ATL, Smyth GK. From reads to genes to pathways: differential expression analysis of RNA-Seq experiments using Rsubread and the edgeR quasi-likelihood pipeline. *F1000Res*. 2016;5:1438.
27. Li X, Cooper NGF, O'Toole TE, Rouchka EC. Choice of library size normalization and statistical methods for differential gene expression analysis in balanced two-group comparisons for RNA-seq studies. *BMC Genomics*. 2020;21(1):75.
28. Qiao L, Gao M, Wang Y, Tian X, Lu L, Liu X. Integrated transcriptomic and metabolomic analysis of cultivar differences provides insights into the browning mechanism of fresh-cut potato tubers. *Postharvest Biol Technol*. 2022;1:188.
29. Wang Q, Wu X, Liu L, Yao D, Li J, Fang J, et al. Transcriptome and metabolomic analysis to reveal the browning spot formation of 'Huangguan' pear. *BMC Plant Biol*. 2021;21(1):321.
30. Chen C, Jiang A, Liu C, Wagstaff C, Zhao Q, Zhang Y, et al. Hydrogen sulfide inhibits the browning of fresh-cut apple by regulating the antioxidant, energy and lipid metabolism. *Postharvest Biol Technol*. 2021;1:175.
31. Miranda C, Irisarri P, Arellano J, Bielsa FJ, Valencia A, Urrestarazu J, et al. Assessment of flesh browning diversity in apple germplasm collections phenotyped by image analysis. In: *Acta Hort.* Int Soc Horticultural Sci. 2023;1362:483–7.
32. Millán-Laleona A, Bielsa F, Aranda-Cañada E, Gómez-Rincón C, Errea P, López V. Antioxidant, Antidiabetic, and Anti-Obesity Properties of Apple Pulp Extracts (*Malus domestica* Borkh.): A Comparative Study of 15 Local and Commercial Cultivars from Spain. *Biology* (Basel). 2023;12(7):891.
33. Palou E, López-Malo A, Barbosa-Cánovas GV, Welti-Chanes J, Swanson BG. Polyphenoloxidase Activity and Color of Blanched and High Hydrostatic Pressure Treated Banana Puree. *J Food Sci*. 1999;64(1):42–5.
34. Luo MR, Cui G, Rigg B. The development of the CIE 2000 colour-difference formula: CIEDE2000. *Color Res Appl*. 2001;26(5):340–50.
35. Sharma G, Wu W, Dalal EN. The CIEDE2000 color-difference formula: Implementation notes, supplementary test data, and mathematical observations. *Color Res Appl*. 2005;30(1):21–30.
36. Sánchez Beeckman M. ColorNameR: Give Colors a Name. A tool for transforming coordinates in a color space to common color names using data from the Royal Horticultural Society and the International Union for the Protection of New Varieties of Plants. CRAN: Contributed Packages. 2021.
37. Meisel L, Fonseca B, González S, Baeza-Yates R, Cambiazo V, Campos R, et al. A Rapid and Efficient Method for Purifying High Quality Total RNA from Peaches (*Prunus persica*) for Functional Genomics Analyses. *Biol Res*. 2005;38(1):83–8.
38. Bolger AM, Lohse M, Usadel B. Trimmomatic: a flexible trimmer for Illumina sequence data. *Bioinformatics*. 2014;30(15):2114–20.
39. Kim D, Langmead B, Salzberg SL. HISAT: a fast spliced aligner with low memory requirements. *Nat Methods*. 2015;12(4):357–60.
40. Daccord N, Celson JM, Linsmith G, Becker C, Choise N, Schijlen E, et al. High-quality de novo assembly of the apple genome and methylome dynamics of early fruit development. *Nat Genet*. 2017;49(7):1099–106.
41. Li H, Handsaker B, Wysoker A, Fennell T, Ruan J, Homer N, et al. The Sequence Alignment/Map format and SAMtools. *Bioinformatics*. 2009;25(16):2078–9.
42. Robinson MD, McCarthy DJ, Smyth GK. edgeR: a Bioconductor package for differential expression analysis of digital gene expression data. *Bioinformatics*. 2010;26(1):139–40.
43. Langfelder P, Horvath S. WGCNA: an R package for weighted correlation network analysis. *BMC Bioinformatics*. 2008;9(1):559.
44. Medina-Rivera A, Defrance M, Sand O, Herrmann C, Castro-Mondragón JA, Delerue J, et al. RSAT 2015: Regulatory sequence analysis tools. *Nucleic Acids Res*. 2015;43(W1):W50–6.
45. Contreras-Moreira B, Castro-Mondragón J, Rioualen C, Cantalapiedra CP, Van Helden J. RSAT: Plants: Motif Discovery within Clusters of Upstream Sequences in Plant Genomes. *Plant Synthetic Promoters*. 2016;1482:279–95. Available from: <http://plants.rsat.eu>.
46. Ksouri N, Castro-Mondragón JA, Montardit-Tarda F, van Helden J, Contreras-Moreira B, Gogorcena Y. Tuning promoter boundaries improves regulatory motif discovery in nonmodel plants: the peach example. *Plant Physiol*. 2021;185(3):1242–58.

47. Ruijter JM, Ramakers C, Hoogaars WMH, Karlen Y, Bakker O, van den Hoff MJB, et al. Amplification efficiency: linking baseline and bias in the analysis of quantitative PCR data. *Nucleic Acids Res.* 2009;37(6):e45–e45.
48. Livak KJ, Schmittgen TD. Analysis of Relative Gene Expression Data Using Real-Time Quantitative PCR and the 2^{-ΔΔCT} Method. *Methods.* 2001;25(4):402–8.
49. Cebulj A, Populin F, Masuero D, Vrhovsek U, Angeli L, Morozova K, et al. A multifaced approach sheds light on the molecular details underlying the mechanism preventing enzymatic browning in 'Majda' apple cultivar (*Malus domestica* Borkh.). *Sci Hortic.* 2023;318:112137.
50. Hamdan N, Lee CH, Wong SL, Fauzi CENCA, Zamri MMA, Lee TH. Prevention of Enzymatic Browning by Natural Extracts and Genome-Editing: A Review on Recent Progress. *Molecules.* MDPI. 2022;27(3):1101.
51. Neves J, Sampaio M, Séneca A, Pereira S, Pissarra J, Pereira C. Abiotic stress triggers the expression of genes involved in protein storage vacuole and exocyst-mediated routes. *Int J Mol Sci.* 2021;22(19):10644.
52. Peenková T, Hála M, Kulich I, Kocourková D, Drdová E, Fendrych M, et al. The role for the exocyst complex subunits Exo70B2 and Exo70H1 in the plant-pathogen interaction. *J Exp Bot.* 2011;62(6):2107–16.
53. Zhao J, Zhang H, Zhang X, Wang Z, Niu Y, Chen Y, et al. The Exocyst Complex Subunit EXO70E1-V From *Haynaldia villosa* Interacts With Wheat Powdery Mildew Resistance Gene *CMPG1-V*. *Front Plant Sci.* 2021;8:12.
54. Eklöf JM, Brumer H. The XTH gene family: An update on enzyme structure, function, and phylogeny in xyloglucan remodeling. *Plant Physiol.* 2010;153(2):456–66.
55. Ishida K, Yokoyama R. Reconsidering the function of the xyloglucan endotransglucosylase/hydrolase family. *J Plant Res.* 2022;135(2):145–56.
56. Kohorn BD, Kohorn SL. The cell wall-associated kinases, WAKs, as pectin receptors. *Frontiers in Plant Science.* *Front Res Found.* 2012;3:88.
57. Wang J, Li F, Zhang X, Sun W, Ali M, Li X, et al. Combined transcriptomic and targeted metabolomic analysis reveals the mechanism of flesh browning in cold stored 'Fuji' apple fruit. *Sci Hortic.* 2023;320:112195.
58. Lian XY, Wang X, Gao HN, Jiang H, Mao K, You CX, et al. Genome wide analysis and functional identification of *MdKCS* genes in apple. *Plant Physiol Biochem.* 2020;1(151):299–312.
59. Czyzewicz N, Nikonorova N, Meyer MR, Sandal P, Shah S, Vu LD, et al. The growing story of (*ARABIDOPSIS*) *CRINKLY 4*. Vol. 67, *Journal of Experimental Botany*. England: Oxford University Press; 2016. p. 4835–47.
60. Gershtater MC, Edwards R. Regulating biological activity in plants with carboxylesterases. *Plant Sci.* 2007;73:579–88.
61. Samuel MA, Salt JN, Shiu SH, Goring DR. Multifunctional Arm Repeat Domains in Plants. *Int Rev Cytology.* 2006;253:1–26.
62. Ahmed MZ, Alqahtani AS, Nasr FA, Alsufyani SA. Comprehensive analysis of the COBRA-like (COBL) gene family through whole-genome analysis of land plants. *Genet Resour Crop Evol.* 2024;71(2):863–72.
63. Sangi S, Araújo PM, Coelho FS, Gazara RK, Almeida-Silva F, Venancio TM, et al. Genome-wide analysis of the cobra-like gene family supports gene expansion through whole-genome duplication in soybean (*Glycine max*). *Plants.* 2021;10(1):1–13.
64. Kumar S, Deng CH, Molloy C, Kirk C, Plunkett B, Lin-Wang K, et al. Extreme-phenotype GWAS unravels a complex nexus between apple (*Malus domestica*) red-flesh colour and internal flesh browning. *Fruit Res.* 2022;2:12.
65. Ge X, Li GJ, Wang SB, Zhu H, Zhu T, Wang X, et al. *AtNUDT7*, a negative regulator of basal immunity in *Arabidopsis*, modulates two distinct defense response pathways and is involved in maintaining redox homeostasis. *Plant Physiol.* 2007;145(1):204–15.
66. Czégény G, Kőrösi L, Strid Á, Hideg É. Multiple roles for Vitamin B6 in plant acclimation to UV-B. *Sci Rep.* 2019;9(1):1259.
67. Meraj TA, Fu J, Raza MA, Zhu C, Shen Q, Xu D, et al. Transcriptional Factors Regulate Plant Stress Responses Through Mediating Secondary Metabolism. *Genes (Basel).* 2020;11(4):346.
68. Sun HY, Zhang WW, Qu HY, Gou SS, Li LX, Song HH, et al. Transcriptomics reveals the *erf2-bhlh2-cml5* module responses to *h2 s* and *ros* in postharvest calcium deficiency apples. *Int J Mol Sci.* 2021;22(23).
69. An JP, Zhang XW, Bi SQ, You CX, Wang XF, Hao YJ. The ERF transcription factor *MdERF38* promotes drought stress-induced anthocyanin biosynthesis in apple. *Plant J.* 2020;101(3):573–89.
70. Boro P, Sultana A, Mandal K, Chattopadhyay S. Interplay between glutathione and mitogen-activated protein kinase 3 via transcription factor *WRKY40* under combined osmotic and cold stress in *Arabidopsis*. *J Plant Physiol.* 2022;271.
71. Xiao P, Feng JW, Zhu XT, Gao J. Evolution Analyses of CAMTA Transcription Factor in Plants and Its Enhancing Effect on Cold-tolerance. *Front Plant Sci.* 2021;12.
72. Singh J, Fabrizio J, Desnoues E, Silva JP, Busch W, Khan A. Root system traits impact early fire blight susceptibility in apple (*Malus x domestica*). *BMC Plant Biol.* 2019;19(1).
73. An JP, Zhang XW, Bi SQ, You CX, Wang XF, Hao YJ. The ERF transcription factor *MdERF38* promotes drought stress-induced anthocyanin biosynthesis in apple. *Plant J.* 2020;101(3):573–89.
74. Zhang L, Zeng Q, Zhu Q, Tan Y, Guo X. Essential Roles of Cupredoxin Family Proteins in Soybean Cyst Nematode Resistance. *Phytopathology.* 2022;112(7):1545–58.
75. Chen X, Wang D, Zhang C, Wang X, Yang K, Wang Y, et al. The Apple Lipoxygenase *MdLOX3* Regulates Salt Tolerance and ABA Sensitivity. *Horticulturae.* 2022;8(7).

Publisher's Note

Springer Nature remains neutral with regard to jurisdictional claims in published maps and institutional affiliations.